Article:
Ibn-Mohammed, T., Randall, C.A., Mustapha, K.B. et al. (7 more authors) (2019) Decarbonising ceramic manufacturing : a techno-economic analysis of energy efficient sintering technologies in the functional materials sector. Journal of the European Ceramic Society, 39 (16). pp. 5213-5235. ISSN 0955-2219

https://doi.org/10.1016/j.jeurceramsoc.2019.08.011

Journal of the European Ceramic Society 39 (2019) 5213–5235

Contents lists available at ScienceDirect

Journal of the European Ceramic Society

journal homepage: www.elsevier.com/locate/jeurceramsoc

Original Article

Decarbonising ceramic manufacturing: A techno-economic analysis of energy efficient sintering technologies in the functional materials sector

T. Ibn-Mohammed[a,b,c,d,h,*], C.A. Randall[d,**], K.B. Mustapha[e], J. Guo[d,f], J. Walker[g], S. Berbano[d], S.C.L. Koh[b,c], D. Wang[h], D.C. Sinclair[h], I.M. Reaney[h,**]

[a] Warwick Manufacturing Group (WMG), The University of Warwick, Coventry, CV4 7AL, UK
[b] Centre for Energy, Environment and Sustainability, The University of Sheffield, Sheffield, S10 1FL, UK
[c] Advanced Resource Efficiency Centre, The University of Sheffield, Sheffield, S10 1FL, UK
[d] Materials Research Institute, The Pennsylvania State University, University Park, PA, 16802, USA
[e] Department of Mechanical, Materials and Manufacturing Engineering, University of Nottingham, Malaysia Campus, 43500, Malaysia
[f] State Key Laboratory for Mechanical Behaviour of Materials, School of Materials Science and Engineering Xi'an Jiaotong University, Xi'an, 710049, China
[g] Department of Materials Science and Engineering, Norwegian University of Science and Technology, NO-7491, Trondheim, Norway
[h] Departments of Materials Science and Engineering, The University of Sheffield, Sheffield, S1 3JD, UK

ARTICLE INFO

Keywords:
Sintering techniques
Ceramics manufacturing
Energy reduction
Energy efficiency
Techno-economic analysis
Investment appraisal

ABSTRACT

The rising cost of energy and concerns about the environmental impact of manufacturing processes have necessitated the need for more efficient and sustainable manufacturing. The ceramic industry is an energy intensive industrial sector and consequently the potential to improve energy efficiency is huge, particularly through the introduction of modern sintering technologies. Although several energy efficient sintering processes have been developed, there is no comprehensive techno-economic analysis which compares and contrasts these techniques. This paper presents a critical review and analysis of a number of sintering techniques and compares them with the recently developed cold sintering process (CSP), including mode of operation, sintering mechanism, typical heating rates, duration of sintering, energy consumption profile and energy saving potential, limitations, key challenges for further development and current research efforts. By using a figure of merit, pounds per tonne of CO_2 saved (£/tCO_2-eq), which links initial capital investment with energy savings, within a framework derived from ranking principles such as marginal abatement cost curves and Pareto optimisation, we have demonstrated that under the scenarios considered for 3 separate functional oxides ZnO, PZT and $BaTiO_3$, CSP is the most economically attractive sintering option, indicating lower capital costs and best return on investment as well as considerable energy and emission savings. Although the current work establishes the viability of CSP as a competitive and sustainable alternative to other sintering techniques, the transition from laboratory to industry of CSP will require hugely different facilities and instrumentation as well as relevant property/performance validation to realise its full potential.

1. Introduction

1.1. Industrial emissions and the quest for reduction

An analysis of sources of emissions by economic sectors indicates that the industrial sector is a key consumer of the global primary energy supply, and therefore a major contributor to global emissions and its associated environmental pollution and impact. For instance, 21% of the economic activities that led to the production of emissions and related pollutants in 2010 was attributed to the industrial sector (Fig. 1a) [1]. This represents a 43% increase in total global emissions from 2005 when the emissions attributed to industrial sector was 14.7%, indicating that the sector is an integral component to addressing energy and environmental pollution issues [2]. The International Energy Agency [3] also reported that between 1990 and 2014, direct GHG emissions in the industrial sector increased by roughly 70%, but during the same time frame, the economic output of the sector increased at a slightly faster pace than its GHG emissions leading to 5% reduction of direct GHG emissions per unit of economic output, Fig. 1b. This suggests that although the sector consumes considerable energy and

* Corresponding author at: Warwick Manufacturing Group (WMG), The University of Warwick, Coventry, CV4 7AL, UK.
** Corresponding authors.
E-mail addresses: t.ibn-mohammed@warwick.ac.uk (T. Ibn-Mohammed), car4@psu.edu (C.A. Randall), i.m.reaney@sheffield.ac.uk (I.M. Reaney).

https://doi.org/10.1016/j.jeurceramsoc.2019.08.011
Received 8 April 2019; Received in revised form 1 August 2019; Accepted 7 August 2019
Available online 11 August 2019

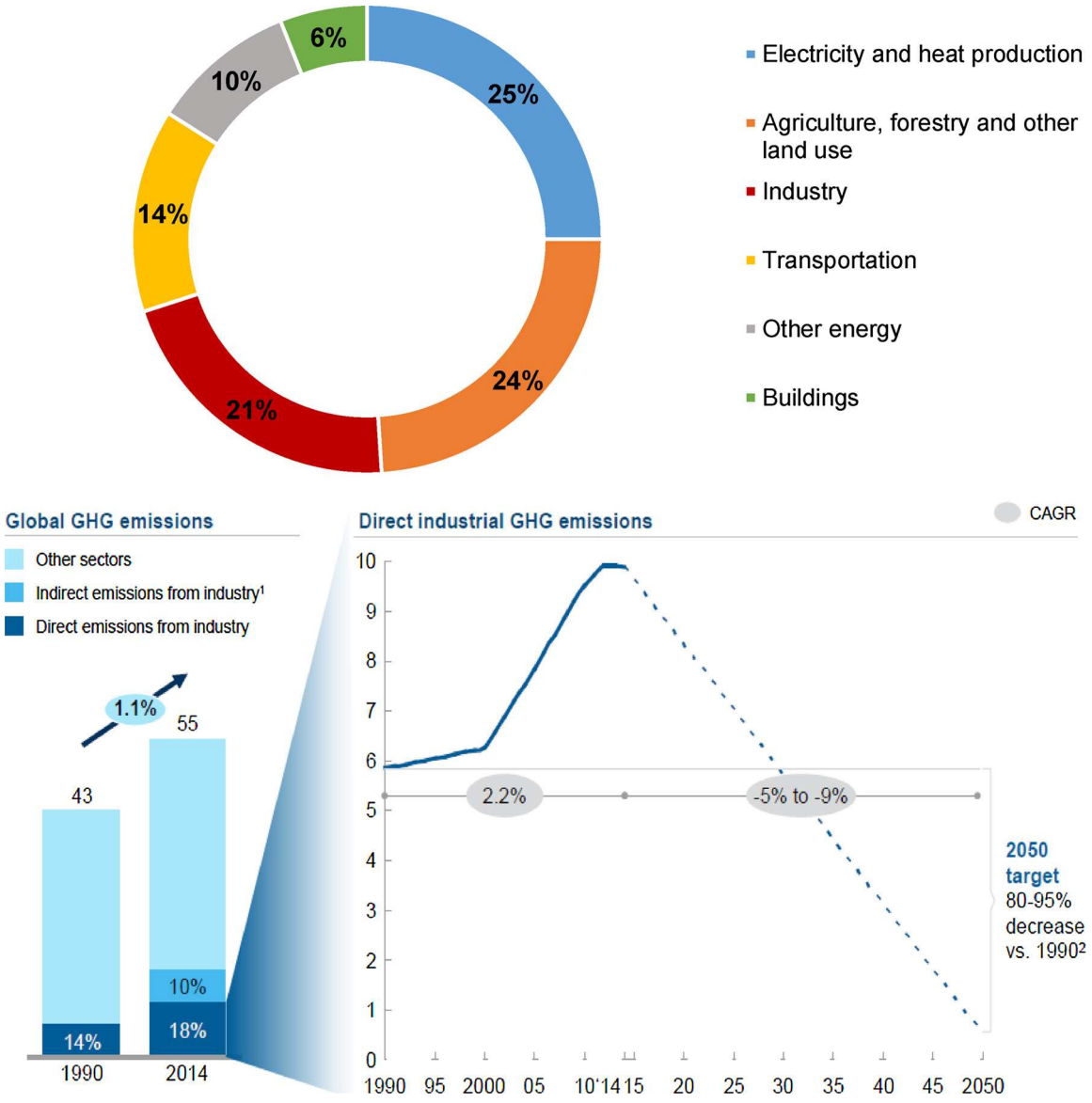

Fig. 1. (a) Global Emissions by Economic Sector. GHG emissions from industry consist mainly of burning of fossil fuels at facilities for energy. It includes emissions from chemical, metallurgical and mineral transmogrification processes not attributed to energy consumption and emissions attributed to waste management activities; (b) emission profile of the industrial sector between 1990 and 2014, indicating emissions, both direct and indirect, will require turnaround from growth to a steep drop to attain 2050 targets. CAGR: Compound Annual Growth Rate.

contributes to high emissions and environmental pollution, it remains key to delivering the global efforts towards a low-carbon economy, whilst contributing to its growth and balance. This is evident, given that much of the economic growth experienced by emerging markets today is triggered by developments in industrial and manufacturing activities that require greater resource inputs, leading to overall increase in the environmental impact of the sector.

As illustrated in Fig. 1b, to achieve significant improvements in the industrial sector, emissions, both direct and indirect, will require turnaround from growth to a steep drop to attain 2050 targets. Given that the industrial sector accounts for 28% of global GHG emissions in 2014, it follows that the set targets cannot be attained without decarbonising the sector. The decarbonisation of the industrial sector is therefore the next frontier after the significant breakthroughs and successes recorded in the building, transport and power sectors, due to the scaling up of decarbonisation technologies. As such, energy efficient and sustainable manufacturing processes based on advanced technologies with reduced energy costs and lower environmental impact have become an important research focus [4–8].

1.2. Energy consumption and CO_2 emissions in the ceramic industry

The conservation of energy is a vital step that must be taken in order to overcome the escalating problems of global energy crisis and environmental impact. One of the energy intensive industrial sectors that has the potential to improve efficiency by leveraging modern energy reduction technologies is the ceramic industry [9]. As such, the sector was given a special attention and consideration towards decarbonisation efforts in the recently published Industrial Decarbonisation and Energy Efficiency Roadmaps to 2050 commissioned by the Department for Business, Energy & Industrial Strategy (BEIS) [10]. As one of humanity's oldest industries through which the greatest and earliest achievements were recorded, the ceramic industrial sector is a future-oriented sector with enormous strategic importance, given its ability to contribute towards the development of a competitive resource-efficient and low-carbon economy in the years ahead [11].

With its expansive array of applications, ranging from consumer goods, construction, through to cutting-edge technologies and manufacturing processes, the ceramic industry is at the forefront of developing high-value and innovative solutions that improve quality of life whilst enabling crucial progress in downstream sectors [10,11]. Indeed, products from the sector play a significant and very often indispensable function in realising energy and resource efficiency in other sectors. By facilitating energy and resource efficiency in all these allied sectors, ceramics play a vital role in the society. In the UK, for example, the sector yielded over four million tonnes of a wide range of products in 2012, whilst contributing a direct value of £1 billion equivalent to its economy [10].

The ceramic industry consumes much energy and by extension high CO_2 emission because it utilises specific chemical and mechanical processes for the conversion of raw materials into a malleable solid, powder or slurry, constituting a large percentage of the energy cost in the overall production cost. Electricity consumption represents up to 30% of the production cost in ceramics processing, although it varies based on product type and cost of fuel [12]. This is particularly the case in the UK where the total emissions attributed to ceramic installations in 2012 is 1.2 Mt CO_2-eq, with fuel costs constituting roughly 35% of total manufacturing costs [10]. Fig. 2 shows the percentage distribution of energy cost attributed to manufacturing cost by industry in Japan, for example [13]. As indicated, the percentage of the ceramic industry (including glass, pottery and cement) is 8.9%. A reduction in energy use and cost can therefore lower the production cost, whilst generating an immediate impact on profit.

As highlighted above, all the subsectors within the ceramic industrial sector are energy intensive given an integral part of the process entails drying followed by sintering at very high temperatures of between 800 °C and 2000 °C [14]. Sintering is a form of heat treatment to which powder compact is subject with the aim of imparting strength and integrity. It is the procedure for compacting and forming a solid mass of material with the aid of heat or pressure without melting to the point of liquefaction. Over 60% of the 10,700 T J consumed by the UK ceramics sector is utilised for sintering [12]. In the quest to reduce the energy consumption, carbon footprint, energy costs, environmental impact and protect world resources, it has been established that traditional firing or sintering process may now become unnecessary for many ceramic materials, given that a broad spectrum of inorganic materials and composites can also be sintered between room temperature and 200 °C, using the cold sintering process (CSP) developed by Randall and co-workers [15–18]. CSP relies on a second phase that facilitates mass transfer for densification, a process that occurs at low temperatures and over much shorter time frames, minutes instead of hours, when a uniaxial pressure is applied [15–18]. Mostly, these phases produce liquids that evaporate during the process. The transient liquid drives the densification via a solution-precipitation process [15–18].

1.3. Research gap and specific objectives

Despite the upsurge in research interests relating to developing low temperature sintering process, techno-economic analyses of CSP alongside existing sintering techniques such as traditional and Spark Plasma Sintering (SPS) is lacking. Understanding the potential techno-economic impact of sintering techniques, manufacturing routes and materials composites is essential, and it is crucial that such an understanding commence at the design stage and/or at laboratory stage, not after they are fully scaled up or used. This research need is addressed in this paper using a robust techno-economic analysis framework derived from ranking mechanisms of marginal abatement cost curve (MACC) and Pareto optimisation. This allows us to classify sintering techniques into those that are able to reduce energy consumption and save money and those that may reduce energy consumption but require a net investment at the level of the laboratory.

Specifically, the objectives of the paper are to: (i) carry out a brief review of a number of sintering techniques to highlight and compare their potential towards energy consumption reduction during ceramic processing; (ii) develop a robust mathematical modelling of energy consumption in parts fabrication via sintering; (iii) establish the viability of cold sintering as a competitive and sustainable alternative to

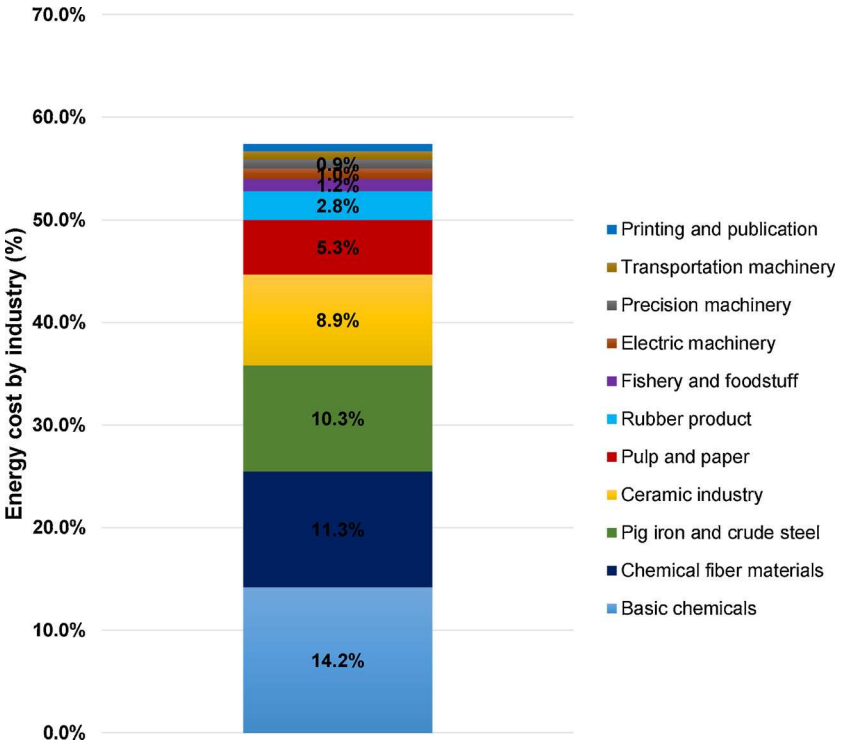

Fig. 2. Distribution of energy cost by industry in Japan [13].

other traditional high temperature ceramic manufacturing techniques, using three functional ceramics, ZnO, PZT and $BaTiO_3$; (iv) develop different scenarios within a techno-economic analysis (TEA) framework to model the identified synthesis and sintering routes as well as energy and mass inputs; (v) establish the cross-over point between cold sintering techniques and other sintering techniques with the view to identify which parameters to be optimised when transitioning from laboratory to the industry; and (vi) establish an appropriate figure of merit that links financial cost with energy savings, for comparing all sintering techniques under consideration. This will lead to the optimal ranking of the cost-effectiveness of each sintering technique with respect to their energy saving potentials.

In light of the above, the remainder of the paper is organised as follows. In Section 2, a critical review of a number of sintering techniques is provided. Detailed mathematical modelling of a generalised energy equation which governs the sintering techniques is provided in Section 3. In Section 4, the overall methodological framework underpinning the techno-economic analysis within a MACC framework and Pareto optimisation principle is provided. In Section 5, the key findings from the analysis are discussed alongside a robust sensitivity analysis, highlighting the implications of the work to novel sintering techniques leading to the limitations as well the summary and concluding remarks in Sections 6 and 7 respectively.

2. Critical review of selected ceramic sintering techniques

The theory of sintering is most accurately used to describe single phase powders sintered through solid state diffusion but in practice, this represent a small portion of sintering activities, given that a number of other sintering techniques entails multiple phases and liquids. Fig. 3 depicts a pictorial representation of sintering techniques in the form of a general categorisation. For a full description of each of the classified sintering techniques, we refer readers to German [19]. The subsections that follow present a review of selected sintering techniques in comparison to cold sintering, including mode of operation and unique attributes, sintering mechanism (i.e. mechanistic details), electrical conditions (i.e. energy consumption profile), typical heating rate, duration of sintering, energy saving potential, limitations, key research and upscaling challenges for further development and current research efforts.

2.1. Conventional or traditional sintering technique

Generally speaking, sintering entails the thermal treatment of powder particles at a temperature which is below the melting point of the main constituent with the view to increase the strength of the particles under consideration by bonding them together [20]. In other words, sintering entails the compacting and forming of a solid mass of material by subjecting it to heat or pressure without melting it to the point of liquefaction. Essentially, the process is used to establish a dense solid mainly aided by thermal energy and/or pressure [19]. Sintering is an integral part of the manufacturing process of functional ceramics given the control it imposes on numerous important properties of the finished product including abrasion resistance, mechanical strength, resistance to water and chemicals, dimensional stability, conductivity and ductility as well as fire resistance [21]. Essentially, the main objective of sintering is to reduce compact porosity with the view to [22]: (i) increasing the contact area of particles; (ii) rounding off points of contact and sharp angles; (iii) ensuring a decrement in the volume of interconnected pores and facilitating the grain growth whilst decreasing the volume of isolated pores.

Conventional or traditional sintering entails the heating of materials at comparatively high temperatures, $T > T_m/2$, where T_m is the melting point, and under not too high pressure, $P < 0.2$ GPa (2.0kBar), across a time frame from minutes to hours. These conditions ensure the adhesion and densification of powder through numerous diffusion dependent processes, including surface and grain boundary diffusion [20]. Depending on the materials under consideration, the sintering temperature range for conventional sintering technique is at high temperatures typically > 1000 °C to facilitate the mass transport processes that allows atoms, cations or molecular groups to diffuse [16]. This mass transport mechanism reduces the surface area of the particulates whilst eliminating porosity [23]. At high temperatures, the fine particles go through numerous changes from particle rearrangement, grain growth and pore elimination. In conventional sintering, energy is transported to the material via conduction and radiation of heat from

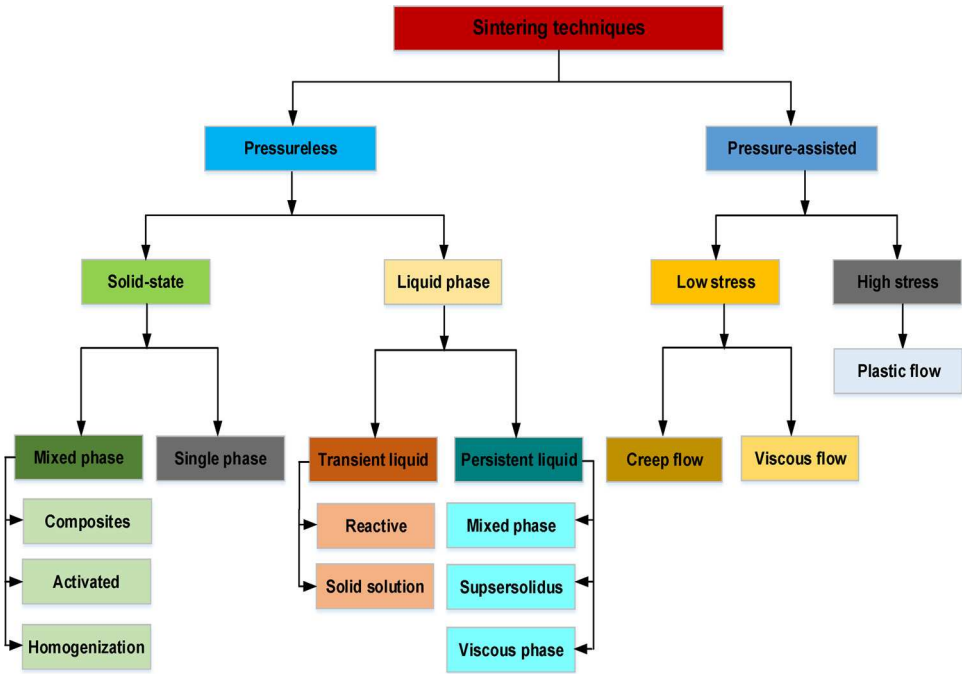

Fig. 3. The classification of sintering differentiated by branches, starting with the application of pressure-assisted vs. pressureless sintering, adapted from German [19].

the surface (i.e. energy transfer is induced by external heating source whereby heat flow is from outside to inside and is not dependent on the materials under consideration) [24].

A major feature of the conventional sintering technique is the high sintering temperature and longer duration needed for the consolidation of the ceramic particles which often leads to extreme coarsening of grains and decomposition of the ceramic, causing the mechanical properties to deteriorate [25,26]. Due to the high melting temperature required for numerous ceramics, conventional sintering is normally accomplished between ˜ 50%–75% of their melting points, as a rule of thumb [27]. For oxides, the temperature at which sintering takes place is typically > 1000 °C and over a few hours, though sintering profiles can extend to days [19,23]. Additionally, the chemical stoichiometry of the end product from this sintering approach may differ due to volatilisation of elements such as Pb, Bi, K and Na or where co-firing of different materials (e.g. electrode-ceramic co-fired MLCCs) are involved, resulting into property and crystal structure deviation triggered by the alteration of defects concentration or intergranular diffusion [28–33].

In an effort to achieve densification at lower temperatures compared to conventional sintering, hot pressing has shown promise, given the improvement of the kinetics of densification and the limiting of grain growth [34,35]. Major disadvantages pertain to the constrained geometry of the final product and the expensive nature of the equipment required [22]. Additionally, in hot pressing technique, the particle container is characteristically heated by radiation from the surrounding furnace by convection of inert gases and external heating elements where applicable. As such, the material under processing is heated by transfer of heat via conduction from the external surface of the container to the particles, leading to slow heating rate and thereby elongating the overall duration for the sintering process [22]. For a full description of conventional sintering technique, we refer readers to German [19] and Bordia et al. [36]. Attempts to lower sintering temperature and by extension the sintering time have led to the development of novel sintering techniques described in the sections that follows.

2.2. Microwave sintering

Microwaves are characterized by wavelengths, 1 cm− 1 mm, corresponding to 300 MHz− 300 GHz and are best known to the public for their strong interaction with water molecules resulting in the development of the microwave oven [37]. Microwaves are key enablers of cellular, radar, and satellite communications facilities [37] but they are also used in the processing of advanced materials via microwave-assisted sintering and heating [38–42]. Developments in this area have focussed on applications such as pharmaceutical [43], material joining [44,45], electronics packaging [46], and polymer curing [47,48]. This section sheds light on the evolution of microwave sintering by focusing on its mechanism, advantages, energy profile, heating rate, and challenges.

A sintering process improves bonding between the particles by minimizing porosity [49]. Yet, the outcome of sintering is often greatly influenced by the underlying mechanism [50]. The traditional sintering process relies on radiant and resistive heating. In this aspect, the heat energy is transferred through thermal gradients from outside to inside of the powder compact [51,52]. In contrast, microwave sintering does not rely on diffusion of heat from the surfaces. Under irradiation, the volume of materials being sintered absorbs microwave energy and then transforms it into heat, with the heat flowing outwardly from inside to outside. The process allows a 100% transformation between electromagnetic and thermal energy, leading to a reduction in sintering time with greater energy efficiency, enhanced reaction, faster sintering rate without cracking, reduced thermal gradients, improved quality of final products, and low environmental impact [53–55]. In microwave sintering, the key parameters are applied field frequency, temperature of the furnace and the concentration as well as the types of elements used for doping [56–58].

In spite of the aforementioned advantages, the microwave sintering technique is not without shortcomings. The technique requires the use of high-end expensive equipment that costs far more than for the traditional sintering. This has severely hampered the broader proliferation of the process beyond exploratory laboratory demonstration set-ups [59]. Moreover, microwave sintering must be carried out inside a microwave applicator with a sophisticated insulating system. This requirement inhibits real-time data collection and monitoring of the interactions of microwaves with different materials [60]. Monitoring and efficient data collection is needed to enhance the process and provide the basis for understanding the properties of a sintered volume arising from the complex interactions of the powder materials with microwave radiation [61]. It is categorized as an environmentally-friendly process and the temperature requirement for microwave sintering varies from moderate temperature range (500℃ − 1000℃) with minimal power consumption to those above 1000 ℃ (with significant power consumption) [62]. Nonetheless, comparisons of the temperature required to obtain fully dense samples is lower compared to conventional sintering [63].

Earlier applications of microwave sintering was predominantly related to the processing of polymers and ceramics starting from the 50 s [41,50,63]. Extension of the method to sintering of metals were initially thought impossible due to the widely-held belief that metals are microwave reflectors [64]. The myth was shattered by a serendipitous experimental observation in 1999 [65]. Subsequent studies following this breakthrough have revealed that powdered metal components as well as various types of metal alloys can indeed be sintered. Processing conditions are typically 2.45 GHz microwave furnace, the most common frequency for sintering applications [63,66]. For further details on the comparison between microwave and conventional sintering techniques, see Oghbaei and Mirzaee [50].

2.3. Spark plasma sintering (SPS)

It was in the 1960s that spark sintering was first researched and patented, with applications in metal powder compaction [22,67]. However, due to enormous equipment cost and the reduced efficiency of the sintering mechanism, its use was streamlined. By mid-1980s to early 1990s, research on the technique reached an advanced stage yielding a new generation known as Plasma Activation Sintering (PAS) and Spark Plasma Sintering (SPS) [22]. SPS is a form of pressure-assisted sintering which utilises low-voltage, pulsed direct current to heat up the materials under consideration [68]. The technique has attracted enormous attention by manufacturing engineers as well as materials scientists given that it guarantees a quick fabrication route to react and consolidate materials in a single processing step [68,69]. These attributes renders SPS an ideal approach for rapid fabrication and characterisation of new compositions to explore the phase of new possible materials [68,69].

With the adoption of SPS, the duration for processing powder materials is significantly shortened whilst improving the overall powder consolidation. As illustrated in Fig. 4, SPS allows heating and cooling at rates > 200 K/min [69] during powder consolidation as compared to the conventional sintering technique with heating rates of between 2–30 °C/min. [68]. Due to the compact geometry of the die and punches within SPS, sintering cycles with heating rates of up to 1000 °C/min have been reported [68]. Additionally, full densification takes only few minutes in comparison to several hours required by conventional hot processing technique [36].

SPS has therefore become particularly useful for performing rapid densification and consolidation of hard-to-sinter ceramics such as nitrides, carbides, borides and other ceramic composites under reduced temperatures [36,68]. The use of SPS has also shown promise regarding the maintenance of the nano and submicrometer structures in

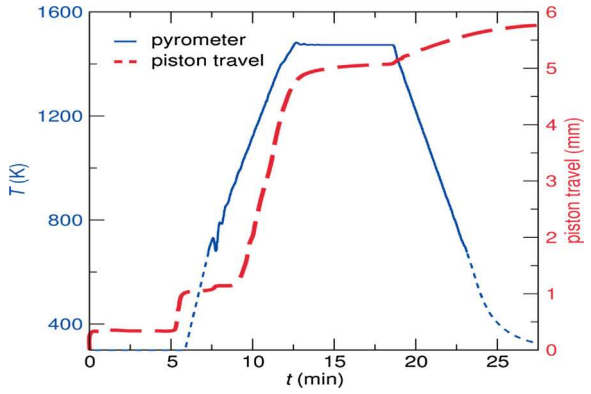

Fig. 4. Illustration of heating and cooling rates of SPS technique, adapted from Gaultois [69].

nanopowders [36,68]. In terms of nanostructured materials processing, SPS has become a sintering technique of choice for the production of dense fine-grained samples from high-melting point ceramic powders and for the preparation of phase-pure materials from precursors [69].

The sintering technique has emerged as an adaptable method of material processing for consolidation and synthesis [36,68]. It facilitates the development of non-conductive and electrically conductive materials at the laboratory scale (with processing cycles including cooling down to room temperature of < 1 h) or the quick fabrication of industrial products [36,68]. The general mode of operation of SPS is based on a mechanical loading with a high-power electrical circuit placed in a pressure, position and temperature-controlled environment as illustrated in Fig. 5. During synthesis, the sample is quickly heated by a pulse current (Joule heating) of the conductive die set while under an applied load with a corresponding increase in temperature when densification is observed [22]. The entire synthesis process including heating, cooling and densification which takes place in < 30 min is possible due to the spark plasma induced by the large pulsed current [22,69]. In SPS, the use of pulsed direct current indicates that the die also serves as a source of heating and that the sample is subjected to heat from both outside and inside [22]. The application of pulsed direct current results in *in-situ* particle surface activation and purification by the spark plasma [22,68]. Accordingly, the heat and mass transfer between the particles is quickly realised.

Due to the complex nature of the different physical phenomenon in SPS, modelling of the process has posed significant challenges and clear insights are only just coming to light about the mechanism involved in

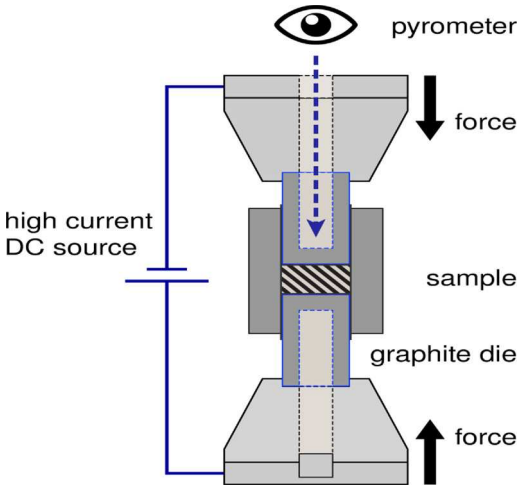

Fig. 5. Basic configuration of SPS illustrating a die set mounted and exposed to a mechanical load and electrical current, adapted from Gaultois [69].

SPS including mechanical, thermal and electrical effects [36,68]. In terms of mechanical effects, the quasi-static compressive stress applied in SPS provides a number of merits such as: (i) better and improved contact between particles which changes the quantity and morphology of those contacts; (ii) enhancements of the prevailing densification mechanisms already available within free sintering (e.g. lattice diffusion, grain boundary diffusion and viscous flow) and (iii) activation of new mechanisms including grain boundary sliding or plastic deformation [68].

From a thermal perspective, a competitive edge offered by SPS is the high rate of heating. When the central densification mechanism (e.g. grain boundary diffusion) has greater activation energy than the coarsening mechanism (e.g. surface diffusion), attaining a fast high-sintering temperature can offer advantages for enhancement of the densification rate whilst retarding microstructure coarsening [68]. Further thermal effects of SPS pertain to increased local temperature gradients or unbalanced distribution of temperature and macroscopic temperature fields yielding thermal stresses [68]. From the perspective of the flow of an electric field, if an electrical conducting raw powder is prepared by SPS, high currents flow through the body as opposed to the surrounding graphite die. In this scenario, interactions between the electric current and the microstructure could yield useful effects such as percolation effects [70,71], Peltier heating [72], electrochemical reaction at the interfaces [73] and electromigration [74].

In summary, SPS is of great importance in the fabrication of bulk nanostructured parts where control of grain growth constitutes a major hindrance [75–77] but further research comparing the mechanisms of SPS and conventional sintering is required under a number of different thermally activated processes including reactive sintering [78–81], densification [74,82,83], crystal growth in both liquid and solid state [67,84] and joining [85–88]. Furthermore, upscaling to large specimen dimensions and improved flexibility based on possible product geometries are also required [36].

Techniques, such as microwave sintering and SPS described are generically termed as Field Assisted Sintering Technology (FAST) [89] in which an electric, magnetic or electromagnetic field are used to enhance densification [90]. Essentially, all sintering techniques based on FAST possess the ability to lessen the temperature for sintering by several hundred degrees as demonstrated when flash sintering was adopted for the fabrication of fine microstructures of $SrTiO_3$ [91] and in some cases, complex multi-layer devices [92].

2.4. Flash sintering

A more recent development in FAST is the so called ‘flash’ sintering. In flash sintering, samples are usually in the form of a bar and two platinum/silver wires wrapped at two ends but the overall configuration depend on the temperature at which sintering is carried out and the ensuing reaction during the sintering operation. The overall configuration is normally suspended inside a furnace within an electric field of intensity of ˜ 1.2 kV/cm applied to the samples through the wires [93]. The electric field enhances the process of densification based on a number of mechanism including field induced effects, Joule heating and interfacial energy changes [94,95]. Overall, FAST depends largely on electric field and the rate of diffusion at grain boundary which boosts diffusion [90]. A detailed description of the effect of electric field on current, temperature profile and other factors such as resistance, dangling bonds at the surface of particles and the energy states of electron in FAST is provided by Heidary et al. [90].

By using the power consumption of FAST or Flash sintering reported by Cologna et al. [96], Heidary et al. [90] were able to calculate overall energy consumption and reported that the use of FAST can contribute to ˜ 49% decrease in energy consumption depending on the materials under consideration. Based on this aggregated energy consumption, Heidary et al. [90] observed that the energy consumed by the furnace constitute the largest impact (i.e. about 6000 times) compared to the

negligible energy consumption via the electric field. Despite the potentials of FAST, it suffers from a number of limitations including complexity of the technique as well as limitations pertaining to geometry given that careful consideration must be ensured such that the electric field is applied in a homogenous fashion [90]. This is particularly important given that grain growth and the rate of densification differs at different electric fields [97,98] – a situation that can lead to densification and grain size inhomogeneity in the samples under consideration as highlighted by Todd et al. [93].

A number of other limitations of FAST/flash sintering have been reported in the extant literature [94,99–101]. As highlighted before, the majority of the energy consumption in FAST is consumed by the furnace that possess large chambers and requires a huge amount of energy to achieve the required temperature. This is further compounded by energy dissipated via thermal conduction and radiation through the walls of the chamber [90]. An ideal energy efficient sintering technology would therefore eliminate the need for a furnace.

2.5. Laser sintering

Laser sintering is utilised for solid powder materials, typically metals and alloys, by targeting the laser directly at points in space based on a 3D model, whilst binding the materials together by raising the powder temperature before the melting temperature (for metals and metal alloys) or above the glass transition point (for polymers), to produce a solid structure [102]. It is one of the latest techniques, adopted mainly to produce models, prototypes and a wide array of products consisting of merging layers of powders [103]. Some advantages of laser sintering include very short processing time, efficient energy usage and localized heat load which decreases the heating temperature of substrates, rendering it an important technique for printable electronics and polymer (flexible) substrates [104]. Laser sintering has been extensively employed for polymers [105] and metals [106] but there are difficulties with respect to ceramics due to their high melting temperature and their brittle nature [90] but recent progress has enabled the viability of producing stable ceramic with very high porosity, programmed architecture of pores and interporous connections [102,107]. The majority of ceramic implants such as hip replacements and knee joint prostheses, dental implants etc. can be manufactured by laser sintering technique provided proper selection of materials and key parameters of the process are guaranteed [103]. The technique has now advanced from virtual prototyping to commercial manufacturing for the development of new materials and products [102]. For instance, high porous materials including chemical foaming, mapping of porous matrix and mechanical frothing have been derived by the technique [107].

There are two subcategories of laser sintering namely selective laser sintering (SLS) and direct metal laser sintering (DMLS) [108]. In terms of laser energy, sintering should be differentiated from melting. For instance, Selective Laser Melting (SLM) adopts a similar concept to SLS but in SLM, the materials are not sintered but melted, allowing for the emergence of different properties such as porosity and crystal structure [109]. SLS is most commonly adopted because of its capability to produce complex parts with complex geometry without the need for additional equipment [102]. It therefore allows for the production of products with physical, mechanical and chemical properties that differs from the properties of the initial material components in a rapid manner and with a greater measure of accuracy [103]. For detailed description of laser sintering technique in terms of principles of operation, sintering mechanism, interactions of ceramic materials with laser beam, characteristics of laser sintered ceramics (i.e. temperature profile of laser sintering, heterogeneities based on hierarchical structures, non-equilibrium phase assemblages and local reactive-sintering), potential benefits, we refer readers to Qian and Shen [102].

A distinct merit of the SLS process is that due to its fully self-supporting nature, it allows for parts to be constructed within other parts (i.e. nesting) with complex geometries that may not be constructed in any other way. As such, the techniques is suitable for moving parts, interlocking parts and other extremely complex designs. Parts produced using SLS have high strength and stiffness as well as very good chemical resistances with various possibilities in terms of finishing (e.g. metallization). Ideal applications of laser sintering include prototypes with mechanical properties such as those based on injection-moulding, lightweight designs using complex lattice structures and one-off or small batch products [102]. Given that the power density is large in laser sintering, the temperature required can be as high as 3000 °C [102]. This high temperature requirement in combination with both high and cooling rates renders laser sintering as a unique technique for sintering ceramics [90]. Accordingly, a number of authors as detailed by Heidary et al. [90] have employed the use of laser sintering for the fabrication of different ceramic materials such as Ta_2O_5, ZrB_2 and $Bi_4Ti_3O_{12}$.

Despite the advantages presented by laser sintering, it poses challenges including large thermal strains due to the high cooling rate that characterise the process [110] and increased residual stress due to the distance between the laser spots and the scanning speed. This can also lead to cracks in some samples and production of amorphous or semi-crystalline structures that are undesirable [90]. Qian and Shen [102] also reported that the high cooling rate may precipitate trapped gas bubble in the end products. In laser sintering technique, there is a fundamental requirement which dictates that the operational parameters of the laser should be painstakingly selected in order to avoid extra heating [111,112]. For metals and polymers, the sintering mechanism and energy consumption profile is well researched and documented [113,114]. For instance, Kruth et al. [115] identified 3 types of bonding during laser sintering of metals including solid state and liquid phase sintering as well as full melting. Similarly, Franco and Romoli [105] submitted that laser sintering technique can be adapted to reach the optimum condition for optimal productivity whilst consuming less energy, although Heidary et al. [90] suggested that their submissions cannot be applied to ceramic sintering processes because DuraForm Polyamide, which possess a melting temperature of 184 °C was adopted in their study. Accordingly, the sintering mechanism and the energy consumption profile of laser sintering of ceramics still requires further research in order to garner a better understanding of the overall benefits of the technique [90].

The consequence of obtaining extremely high temperatures of SLS within a very short time precludes thermodynamic equilibrium which may affect the phase transition sequences [116] and influence the local effective partial pressure of the ambient gas [116]. This is particularly important during the introduction of oxygen or nitrogen, given that the partial pressure of oxygen affects the thermodynamic equilibrium of oxidation processes and can lead to the reduction of sintered material [116]. Overall, the transition from laboratory to market for laser sintering technique for ceramic processing will be dictated through a better understanding of the interactions between laser materials and improved control of the structural heterogeneities [102]. Research efforts are also required to control the residual thermal stresses whilst ensuring that dimensional tolerances are achieved at the micron levels [102]. Addressing these fundamental limitations will widen the scope of application of laser sintering for products with huge commercial value.

2.6. Fast-firing sintering

Fast-firing sintering is a technique that is employed as a means of obtaining high density and fine grain sized ceramic materials and it involves subjecting the ceramic material under consideration to a sintering temperature zone across a short period of time [117]. In fast-firing sintering technique, the rate of densification is exponentially reliant on the activation energy of grain growth. As such, if the densification activation energy (ΔH_d) is greater than the grain growth activation energy (ΔH_g), then the process of densification occurs at a faster

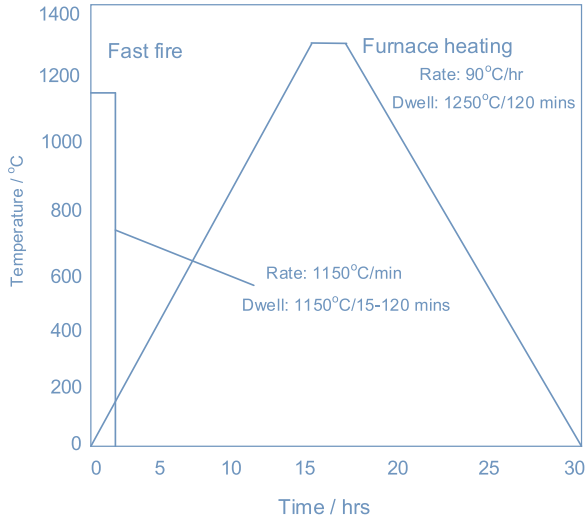

Fig. 6. Illustration of large reduction in processing time by using the fast firing sintering approach.

rate than grain growth above a critical temperature [117]. Hsueh et al. [118] also reported that during fast-firing sintering, the high temperature gradient within the ceramic could cause an upsurge in the rate of densification. Higher densification can be attained faster with a corresponding shortening of the holding time.

In comparison to traditional furnace heating, fast-firing sintering can considerably reduce the processing time. This rapid processing time offers a number of potential merits including [117]: (i) the establishment of fine grain sized materials with potentials for improvement in dielectric and mechanical properties; (ii) drastic reduction in the energy consumed by the furnace whilst allowing for continuous processing; (iii) reduction in material loss (e.g. lead oxide which frequently occur in lead-based materials) held at high sintering temperature over long durations. Fig. 6 illustrates a huge reduction in processing time when fast-firing sintering is adopted.

Using fast-firing sintering, the density of a number of ceramic materials including lead zirconate titanate (PZT) [117–119], Al_2O_3 [120], $BaTiO_3$ [121], Y_2O_3-doped ZrO_2 [122,123] have been shown to increase. For detailed review on fast firing sintering technique see Klein and Hotza [124] and García et al. [125]. Heidary et al. [90] concluded that in a conventional furnace, the reduction in energy consumption is considerable for a slight increase in heating rate which can be achieved by improving the furnace's heating power, through the design of improved heat transfer strategies, by adopting materials that are more thermally insulative and or heat recovery techniques [126,127].

Despite the advantages offered by fast-firing technique, it suffers from a number of limitations. For instance, the notion of increasing heating rate with the view to enhance densification may not be applicable to all ceramics. An example of such instance was extensively illustrated by Rahaman [128] using MgO powder as a case study given that its ΔH_g is between 360 and 450 kJ/mol but the ΔH_d is between 150 and 500 kJ/mol, for which the Mg^{2+} diffusion possess the slowest rates. Furthermore, with the sintering front, the heating rate would be constrained, as described by García et al. [125] who concluded that inhomogeneous densification (i.e. the rise in the amount of pores from the surface toward the inside of the sample) could result if the quantity of heat transfer within the samples is not sufficient to withstand the advancement of the sintering front. As such, fast firing is appropriate for small parts and/or thin wall sections because the heating rate is further constrained when large parts with intricate geometry are being sintered due to different rate of shrinkage which generates internal strain [90].

2.7. Liquid-phase sintering

Liquid phase sintering (LPS) is a sintering strategy employed for producing high performance, multiphase components from powders [129,130]. It is widely employed to consolidate metallic powders and ceramics into final shapes [131]. The technique is simple and effective and has the capability of reducing sintering temperature and by extension energy consumption [90]. It entails sintering under conditions in which solid particles coexist with a wetting liquid (i.e. incorporating a phase into the particles with the aid of low melting temperature) [90,129]. During the process of sintering, the secondary phase melts, enhances flow between the particles whilst facilitating particle rearrangement and diffusion process [90]. Essentially, during LPS, densification is based on rearrangements and change of shape of solid constituents [131]. LPS offers a number of advantages including low sintering temperatures, rapid densification as well as high final densities yielding microstructures that can provide physical or mechanical materials properties that are higher than solid state sintered materials [131]. For detailed description of the underlying mechanism, modes of operations and potential future research area for advancing the LPS, we refer readers to Kaysser and Petzow [131] and German et al. [129].

Different forms of LPS have been applied to an extensive array of engineering materials including connecting rods in engine of automobiles and high-speed metal cutting inserts [129]. The technique has also been employed in the fabrication of a number of ceramics with the view to lowering the sintering temperature. For instance Kimura et al. [132] demonstrated the relationship between the sintering temperatures of $BaTiO_3$ powders whilst using concentrated of Li_2CO_3 as a sintering aid to reduce sintering temperature from 1300 °C to 1000 °C. A summary of a number of materials systems for sintering aids employed for the overall lowering of sintering temperature of LPS is provided by Heidary et al. [90] who concluded that none of the materials systems employed decreased the sintering temperature below 900 °C. However, the application of LPS in varistors based on ZnO, where Bi_2O_3 powder with a melting point of 817 °C was employed as a sintering aid for sintering ZnO powders have been reported [90]. Accordingly, Bi_2O_3 offers advantages in terms of lowering sintering temperature without compromising very good electrical properties [90].

2.8. Cold sintering

For reasons discussed above and outlined in refs [16,133], there is still an industrial need to devise novel sintering technology at temperatures/energy consumption much lower than currently achievable. Cold sintering allows ceramic particulates to be densified at extremely low temperatures of < 300 °C, whilst maintaining low grain size in comparison to conventional sintering technique for typical oxide materials [15,16,134]. The concept of cold sintering was first introduced by Gutmanas et al. [20,135–138] whereby the temperature at which a particular material is sintered is as low as room temperature with densification induced by plastic flow of the particles at 4 GPa. The concept was adjudged successful when applied to metallic powders and composites including cobalt, aluminium, copper, iron, niobium, tantalum and some compounds such as CdTe, MgO, NaCl to mention a few [20]. However, the densification process described by Gutmanas et al. [20,135–138] is solely based on plastic deformation under high pressure with no interdiffusion, which limits the technique to metal and plastic due to the brittle nature of the ceramics and glass [20,90,139]. Liao et al. [140] reduced the particle size of alumina to 18 nm with the view to increasing deformability and obtained samples > 80% dense at 8 GPa at room temperature followed by a post-press anneal at 460 °C, yielding an improved density of > 98%. This was a significant improvement in sintering temperature when compared to conventional sintering which normally occurs at ˜1450 °C. As thermodynamically demonstrated by Liao et al. [140], pressure can allow the prevention of grain growth whilst enhancing densification. As such, the combined

effect of plastic flow and inter-diffusion of particles with an arrested grain growth can lead to development of products with high relative density [90,140].

Densification of ceramics under hydrothermal conditions has also been attempted but did not attract the requisite attention across the entire ceramic community [139]. For example: Roy et al. [141] produced cementitious materials with very high strengths; Hirano and Somiya [142] studied hydrothermal reactions for the densification of basic oxides such as Cr_2O_3 and Anagisawa et al. [143], Yamasaki et al. [144] and Kim et al. [145] have all demonstrated pressing under hydrothermal conditions for the densification of materials such as fly ash, cement and hydroxyapatite. It is important to note that cold sintering technique differs from hydrothermal synthesis. Hydrothermal synthesis make use of phase reactions for the crystallisation of anhydrous materials from solution under sealed reaction vessels [146–148]. Hydrothermal hot pressing and reactive hydrothermal sintering can cause solidification but the product yield are usually porous [146]. However, cold sintering is densification with or without phase reactions as discussed in the succeeding paragraphs [133].

FAST or Flash sintering [96], microwave sintering [24,50], spark plasma sintering [85,149–151], rate-controlled or fast sintering [152], two-step sintering [153] and high-pressure sintering [154] have all thus been utilised in attempts to reduce sintering temperature and consequently energy consumption. Combinations of these techniques have also been attempted [155], all of which have made giant strides towards attaining lower sintering temperature profile, although the reduced temperatures are still typically confined to > 400 °C. However, inspired by research conducted at Tokyo Institute of Technology [156] and at the University of Oulu on lithium molybdate ceramics [157], a novel sintering technique [17] has recently emerged capable of densifying ceramics at < 300 °C from Randall and co-workers at the Pennsylvania State University, USA. Termed the Cold Sintering Process (CSP) [27,133] to distinguish it from high pressure sintering, an increasing number of ceramics and composites can be fabricated at up to 1000 °C lower than their conventional sintering temperatures.

In CSP, diffusion between particles is improved by adding a transient solvent to the powder and easily obtainable pressures of ~350 MPa are required instead of 8 GPa inpreviosu cold sintered ceramics. CSP provides a new route for ceramic fabrication in several ways: (i) aiding new materials discovery through integration of materials that are normally not co-sintered, such as polymers and metals [16]; (ii) reduction in energy consumption towards attaining a decarbonised ceramic sector; (iii) compatibility with multilayer device fabrication technology such as screen printing and tapecasting and (iv) integration of materials that react chemically, undergo decomposition or exhibit volatile behaviours [158].

The range of materials/composites that have been successfully fabricated using CSP include nanomaterials, quantum dots, polymers, inorganics, biomaterials, liquid crystals, 2-D materials, Metal-Organic-Frameworks (MOFs) and phosphors [158]. CSP also covers a wide array of chemical variations and crystal structures including binary and quinary compounds such as phosphates, oxides, iodides, fluorides, chlorides and carbonates [158] in applications such as prospective thermoelectrics, microwave dielectrics, Li-cathode materials, ferroelectrics, piezoelectrics, semiconductors, metallic oxide conductors, ionic electrolytes, and refractory materials [158]. Specifically, CSP has been demonstrated on $BaTiO_3$ [15,159], ZnO [134,139], V_2O_5, [16,17] ZrO_2 [160], Li_2MoO_4 [18,133], $NaNO_2$, [27] $K_2Mo_2O_7$, [133] $Na_2Mo_2O_7$, [133] PZT [161], KH_2PO_4 [27] and many more, whilst attaining density ranging across 90–98%. CSP can be thought of as a derivative of liquid phase sintering given that both techniques utilises liquid phase to enable mass transfer during sintering. A clear distinction between the two techniques lies in the fact that within a LPS, a molten phase with high temperature enhances the diffusion processes but within CSP, such phases are replaced by a solvent and high pressures [133]. Fig. 7 depicts the mechanism and possible routes for different types of materials based on CSP.

CSP involves the following steps [16,27,133]: (i) uniform moistening of the ceramic powders with a small quantity of aqueous solution (e.g. water and/or acidic solution). This allows for the decomposition of the solid surface, whilst accelerating the dissolution and transport kinetics and ensures that a controlled amount of liquid phase is intentionally introduced at the particle-particle interface; (ii) within certain temperatures and/or pressure regimes, the solid particles pass through the process of particle re-arrangement with the aid of the aqueous liquid phase followed by densification through dissolution-precipitation. This precipitation emanates from a supersaturated solution that epitaxially grows on the surfaces of the particles. In the solution-precipitation process, ionic species and/or atomic clusters transport to the contact to allow for the reduction of local surface curvature of the particle; iii) minimisation of the excess surface free energy and iv) reduction in porosity, yielding materials in dense solid forms [17].

Variables in CSP include particle size, quantity of water addition, pH level and addition of solute, amount of pressure applied, sintering temperature, holding time and heating rates can impact the process of sintering under CSP conditions [133]. Essentially, CSP offers a simple, effective and energy-saving strategy for the fabrication of a number of materials and device development given that it successfully eliminates furnace requirements and high temperatures [90]. The energy consumed during CSP can be attributed to (i) the energy required to heat up the dies, evaluated through the monitoring of voltage and current profile during the process; and (ii) energy required for pressing the powders which can be derived by calculating the work done (i.e. the energy expended) by multiplying the force (F) applied (which is a function of pressure (P) and area (A) of the pellet) by the displacement (d) which is the difference in thickness of the pellet before and after the cold sintering process [90].

At the laboratory level, CSP is well-established, however, there are still questions regarding water evaporation processes, densification mechanism and amorphous grain boundaries [90]. There are other challenges of CSP that exist from a scientific and industrial perspective. Specifically an understanding of the dynamic nature of the process is still a challenge with optimisation of grain size and morphology, particle size distribution, die sealing, rate of pressure application, and liquid phase viscosity required [158]. Most significantly, the transition from laboratory to industry will require a hugely different facilities and infrastructures as compared to conventional sintering [158]. Furthermore, statistically relevant property/key performance validation on the industrial side will be required by the ceramic processing community but strategies that involve lower uniaxial pressures and injection moulding would render CSP even more appealing [158].

To compare the energy consumption profile of different sintering techniques, it is important to have a deep understanding of the processes in terms of how they are governed by mass transfer mechanism. Accordingly, a description of the modelling of energy consumption in parts fabrication via sintering is presented in the next section.

3. Modelling of energy consumption in parts fabrication via sintering

Here, we present a detailed description of how a generalised equation governing electrical energy consumption during sintering process is developed. At the molecular level, sintering processes are governed by mass transfer mechanism, and a molecular level modelling of the process offers detail computational information about mass transfer related events such as densification and grain growth [162,163]. However, the molecular level modelling of the sintering processes has a burdensome computational cost for making inferential decision about energy consumption in the rising number of emerging sintering techniques being promoted to mitigate energy and environmental concerns for advanced ceramic processing. In this spirit, an

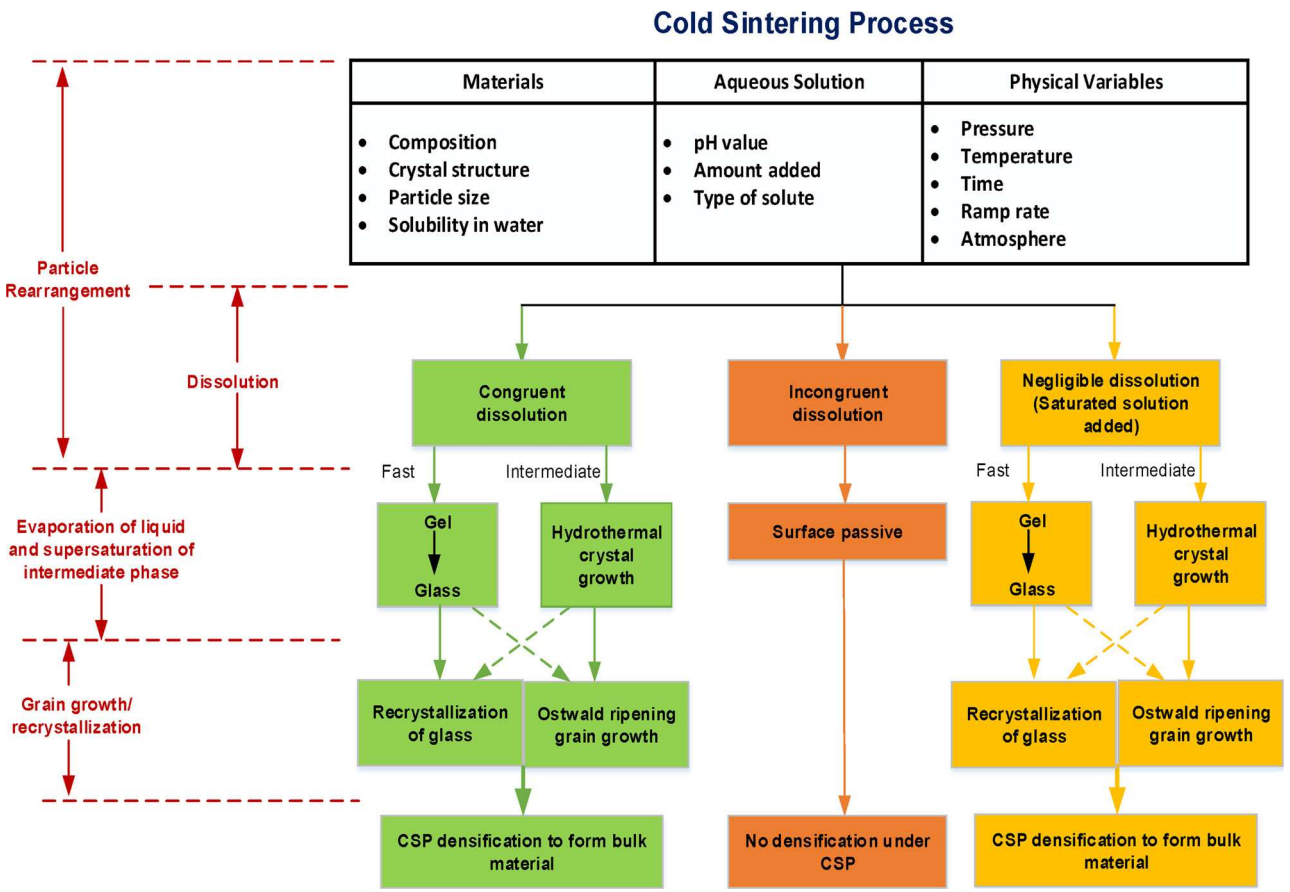

Fig. 7. Fundamental mechanism and possible routes for different types of materials based on CSP. Adapted from Guo et al. [27].

alternative approach is necessary if we are to truly understand the difference between these distinct sintering techniques.

Focusing on cold sintering and the traditional sintering processes as representative examples in this study, we deployed a continuum-level approach, anchored on the concept of transport theorem to: (i) formulate the analytical expression relating important variables that influence the energy consumption pattern of these two types of sintering processes; and (ii) establish a simple process-dependent generalized expression for the energy consumption in these two processes. A calculated choice is made to focus the modelling procedure on the traditional sintering technique (being the dominant sintering method) and the cold sintering technique, which has been demonstrated to have a much lower energy consumption profile, in principle. Commentaries on the differences between these two processes have already been explored in earlier studies [133,159]. For the purpose of modelling, we consider two layers to offer a quantitative appraisal of the macroscopic energy-related events in the two sintering processes. In Section 3.1, we explore the local energy transport within a minuscule control volume of the two processes, while Section 3.2 considers the energy consumption at the level of the chamber.

3.1. Analytical model of local energy transport in sintering processes

Let us consider the simplified schematics of two chambers for part fabrication by means of cold and the traditional sintering processes shown in Fig. 8(a) and (b), respectively. The volume of materials in each chamber is divided into sintered and unsintered regions. With this in mind, we pick an arbitrary small chunk of material and designate this as a control volume. Primarily, the control volume, enclosed by an arbitrary surface boundary shown in each of Fig. 8(a) and (b), surrounds a material point in the sintered region. Furthermore, we label, as revealed in Figs. 8(c) and (d), the size of the control volume as V_{cs} and V_{ts} for cold and traditional sintering process, respectively.

At this juncture, it is necessary to highlight a number of points that underpin the following model for the local energy transport:

- V_{cs} is from a chamber with a global volume V_1, while V_{ts} is from a chamber with a global volume V_2;
- Process constrain dictates that V_1 (for cold sintering) is always less than V_2 (for traditional sintering);
- Both cold sintering and traditional sintering processes are facilitated by particle diffusion, which in turn is aided by heat transfer mechanism to enable powder sintering;
- Conduction is taken to be the dominant heat transfer mechanism within the volume being sintered. This rests on the fact that heat conduction supersedes thermal loss or gain by surface transfer through convection.

Further to the above, it is noted that notwithstanding the type of the sintering process, the heat transfer analysis of each of the two control volume stipulates the satisfaction of this energy balance:

$$\dot{E}_{inf} + \dot{E}_{gen} = \dot{E}_{out} + \dot{E}_{cin} \tag{1}$$

where $\dot{E}_{inf}$ and $\dot{E}_{out}$ refer to the rate of energy flow into and out of the control volume, while $\dot{E}_{gen}$ and $\dot{E}_{cin}$ symbolize the rate of generated energy (mostly by internal sources) and rate of change of internal energy of the control volume, respectively.

For brevity sake, we now restrict ourselves to the control volume in the cold sintering process, and consequently proceed with the heat conduction domain shown in Fig. 8(c). Based on the concept of transport theorem and the Eulerian framework (in which the control volume is fixed with reference to an inertia frame of reference), we pre-suppose

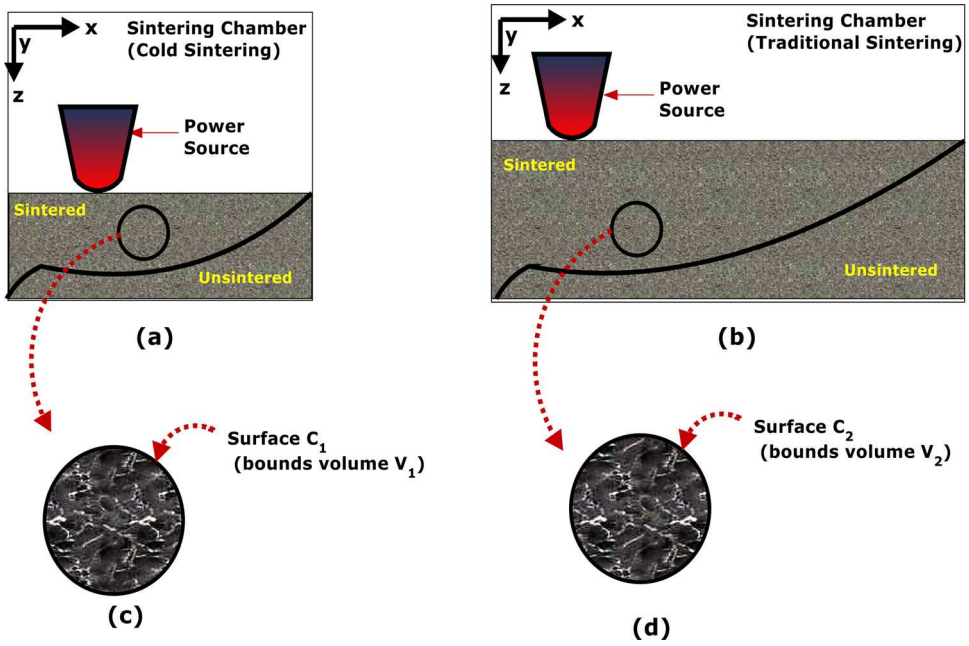

Fig. 8. Schematics of sintering chambers and isolation of control volume: (a) cold sintering; (b) traditional sintering; (c) control volume V_{cs}; (d) control volume V_{ts}.

the process generates a volume density of heat energy u transported through the control volume V_{cs} and endowed with a heat flux density $\boldsymbol{q}(\boldsymbol{x}, t)$. Clearly, the amount of heat energy in V_{cs}, denoted as $U(t)$, can be estimated as:

$$U(t) = \int_V u(\boldsymbol{x}, t) dV_{cs} \tag{2}$$

The time rate of change of the heat energy $U(t)$, at a specific spatial position $\boldsymbol{x}$, is thus:

$$\frac{dU}{dt} = \frac{d}{dt}\int_V u(\boldsymbol{x}, t) dV_{cs} = \int_V \frac{du(\boldsymbol{x}, t)}{dt} dV_{cs} \tag{3}$$

The confluence of the principle of energy conservation and the balance law stated in Eq. (1), necessitates that the time rate of change of $U(t)$ be equated to the addition of the amount of flux through the surface boundary C_1 (surface of the control volume V_{cs} as shown in Fig. 8c) and the generation of heat in V_{cs} (by a source Q). Consequently, we have:

$$\frac{dU}{dt} = -\int_S \boldsymbol{q}.\ \boldsymbol{n}\, dC_1 + \int_V Q\, dV_{cs} \tag{4}$$

where $\boldsymbol{n}$ denotes an outward normal of unit length contributing to the outward flux through surface C_1. To harmonize the integration operations, the first integral in Eq. (4) is transformed using the Gauss theorem, leading to:

$$\frac{dU}{dt} = -\int_V \nabla.\ \boldsymbol{q}\, dV + \int_V Q\, dV_{cs} \tag{5}$$

We re-write Eq. (5), bearing in mind Eq. (3), as:

$$\int_V \left[\frac{du}{dt} + \nabla.\ \boldsymbol{q} - Q\right] dV_{cs} = 0 \tag{6}$$

At this point, we take the amount of heat to be a function of temperature, and as earlier stated we have adopted the Eulerian framework (where the control volume is fixed). Therefore, $u = u(T, t)$ and one may then transform Eq. (6) as:

$$\int_V \left[\frac{du}{dT}\frac{\partial T}{\partial t} + \nabla.\ \boldsymbol{q} - Q\right] dV_{cs} = 0 \tag{7}$$

If the control volume is held constant, the derivative of heat with temperature (du/dT) amounts to specific heat at constant volume (c_v), a well-known thermodynamic material property [164]. Further, in one-dimension, $\nabla.\ q = \frac{\partial q_z}{\partial z}$. Thus:

$$\int_V \left[c_v\frac{\partial T}{\partial t} + \frac{\partial q_z}{\partial z} - Q\right] dV_{cs} = 0 \tag{8}$$

The arbitrariness of the control volume allows:

$$\left[c_v\frac{\partial T}{\partial t} + \frac{\partial q_z}{\partial z} - Q\right]_{cs} = 0 \tag{9}$$

A relation between the heat flux and temperature is provided by the simplified one-dimensional Fourier's law for conductive heat flow (i.e. $q_z = -k dT/dz$) [165]. With this, the differential equation governing the local energy transport within the control volume is obtained as:

$$c_h\frac{\partial T}{\partial t} - \frac{\partial}{\partial z}\left(k\frac{dT}{dz}\right) = Q \tag{10}$$

where k is the axial thermal conductivity (W/mK). A closer examination of Eq. (10) shows that it has a first-order time derivative (which requires a single initial condition) and a second-order spatial derivative (which demands two essential boundary conditions). The solution of Eq. (10) therefore requires the following initial and boundary conditions:

$$T(z = \bar{z}, 0) = \bar{T};\ -k\frac{\partial T}{\partial z}\bigg|_{z=0} = \bar{q} \tag{11}$$

where $\bar{T}$ and $\bar{q}$ are the specified temperature (ambient temperature, for instance) and heat flux, respectively.

In principle, although we have arrived at Eqs. (10) and (11) by using the control volume from Fig. 8(c), the established equations do not have any explicit dependence on volume. Hence, the same set of equations could have been obtained by using the arbitrary control volume from Fig. 8(d). Nevertheless, these equations still offer a means for quantitative comparison between the two sintering processes. First, the underlined derivative in Eq. (10) represents the time history of temperature distribution. Observations from previous studies have revealed that cold sintering has a much lower temperature range per unit time compared to the traditional sintering process [139]. Second, the cold sintering process has a smaller $\bar{q}$ (the boundary condition in Eq. (11))

when compared with the conventional sintering process. This latter point enables the cold sintering process to offer a non-negligible gain in energy efficiency [16,133]. To put things in perspectives, $\bar{q}$ is the flux boundary condition, which is governed by the specific thermal power of the radiating power source.

Now, assuming the sintering process is a laser-based process, then the heat flux immediately below the laser source will be a function of the laser power, spot diameter of the laser beam and the scanning speed (v). However, at some distance away from the source, the boundary condition is governed by the Newton's law of cooling. For the traditional sintering process, the Newton's law of cooling will be:

$$-k\frac{\partial T}{\partial z}\bigg|_{z=0} = h_{tsp}[T_{surf} - T_{air}] \tag{12}$$

where h_{tsp}, T_{surf} and T_{air} are the convective heat transfer coefficient, air-solid interface temperature, and ambient air temperature respectively. Meanwhile, since the cold sintering process is aided by a transient fluid which is different from air, its corresponding Newton's law of cooling will be:

$$-k\frac{\partial T}{\partial z}|_{z=0} = h_{csp}[T_{surf} - T_{solv}] \tag{13}$$

where h_{csp}, T_{surf} and T_{solv} are respectively, the cold sintering convective heat transfer coefficient, the interface temperature between the cold sintering transient solvent and the sintered solid, and the temperature of the transient solvent, deployed to assist diffusion growth in the cold sintering process. In a hydrothermal-assisted cold sintering, for instance, the process makes use of water as the transient fluid [15]. The convective heat transfer coefficient of water is almost 50 times that of air [166]. Therefore, the magnitude of the heat flux, and hence power consumption, is less in the cold sintering process.

3.2. Effect of production yield and sintering chamber size on energy consumption

In Section 3.1, the quantitative information about the energy consumption was based on the consideration of a control volume within the chamber. As such, the mathematical model was derived without a discussion of the effect of chamber size and production yield on the rate of heat generation. In this section, these two factors are considered and we reveal how V_1 and V_2 (volume of sintering chambers) are related.

Let $\dot{Q}_{gcs}$ and $\dot{Q}_{gtsp}$ be the time rate of heat generated internally per V_1 and V_2, respectively. Then:

$$\frac{dQ_{gcs}}{dt} = \dot{q}\,V_1;\ \frac{dQ_{gV_2}}{dt} = \dot{q}\,V_2 \tag{13a, b}$$

where $\dot{q}$ is the rate of heat generated in duration dt per unit volume. The amount of thermal energy generated (Q) can thus be obtained as:

$$Q_{gcs} = \int_{t_1}^{t_2} \dot{q}\,V_1\,dt;\ Q_{gtsp} = \int_{t_1}^{t_2} \dot{q}\,V_2\,dt \tag{14a, b}$$

where $\dot{q}$ is equivalent to thermal power generated per unit volume (P_g), therefore, a generic expression for heat generated within each sintering chamber takes the form:

$$Q = P_g V\,(t_2 - t_1) \tag{15}$$

Applying Eq. (15) to each of the sintering process, one obtains:

$$Q_{gcs} = P_{gcs}\,V_1\,\tau_{cs} = P_{gcs}\frac{m_f}{\rho}\tau_{cs} \tag{16}$$

$$Q_{gtsp} = P_{gtsp}\,V_2\,\tau_{tsp} = P_{gtsp}\frac{m_f}{\rho}\tau_{tsp} \tag{17}$$

where ρ, m_f and τ_{cs} denote density, total mass of the feedstock material being sintered and the duration of the sintering process. Now, since the sintering process may be such that only a fractional mass m_y can be processed at a time, as is true for the cold sintering process which requires multiple sintering runs, then it is convenient to normalize the energy terms. Consequently, for further simplifications, we introduce a unifying term called specific power consumption (κ), where $\kappa = P_g/\rho$, and having a unit of W/Kg, and then re-format Eqs. (16) and (17) in terms of energy per kilogram $\tilde{Q}_{gcs}$ and $\tilde{Q}_{gtsp}$ for the cold and traditional sintering process:

$$\tilde{Q}_{gcs} = \kappa_{cs}\,\tau_{cs}\frac{m_f}{m_y} \tag{18}$$

$$\tilde{Q}_{gtsp} = \kappa_{tsp}\,\tau_{tsp}\frac{m_f}{m_y} \tag{19}$$

In instances where the processing of a given material using cold sintering requires further processing known as annealing as in the case of materials such as PZT and $BaTiO_3$, Eq. (18) can be expanded upon as follows:

$$\tilde{Q}_{total} = \kappa_{cs}\,\tau_{cs}\frac{m_f}{m_y} + \kappa_a\,\tau_a\frac{m_f}{m_y} \tag{20}$$

where on the one hand $\tilde{Q}_{total}$ is the normalized total consumed energy in Joule/kg, while $\kappa_a\,\tau_a$ represents the specific power consumption in the duration of the annealing process.

3.3. Understanding the competitive edge of cold sintering beyond laboratory conditions

As highlighted in Section 2.8, cold sintering process offers tremendous energy saving potential compared to other well-established sintering techniques for ceramic processing. For instance, Heidary et al. [90] reported that the thermal energy consumed due to the sintering of $BaTiO_3$ powder can significantly reduce from 2800 kJ/g using conventional sintering, to 2000 kJ/g based on liquid phase sintering, 1050 kJ/g using FAST sintering, 540 kJ/g with microwave sintering, through to 130 kJ/g for fast-firing, to a very low thermal energy of 30 kJ/g for the CSP. A figure of merit termed "Normalized Excess Energy", was adopted by the authors as a first order approximation for the comparison of the energy savings potential of various to sintering techniques. On a gram by gram basis under laboratory conditions, the submissions by the authors in terms of the superiority of cold sintering process over other types of sintering techniques is valid. However, if the process is scaled up to sinter higher quantities of ceramic materials, there is a cross-over point during which the competitive edge of cold sintering process may become diminished.

To drive home the point, an example based on comparison between energy consumption during cold sintering process (CSP) and conventional/traditional sintering (TSP) of ZnO is used. Assuming 1 kg of ZnO was sintered using CSP and TSP based on the following scenario in the laboratory. CSP: 100 g (equivalent to 1 press) of ZnO was sintered 2 h at 120 °C, resulting in 10 parts for the 1000 g, using sintering equipment with a power rating of 1.8 kW; TSP: 100 g of ZnO pressed for 2 min with an equipment of power rating 1.8 kW and then sintered at 1400 °C for 7 h, yielding 10 cycles for the 1000 g (i.e. 10 parts for the 1 kg), power rating of equipment is 5.5 kW. Based on this laboratory sintering scenario, CSP consumes 12.96 MJ (3.6 kW h) per press, resulting in 36 kW h for the entire 10 presses. On the other hand, TSP consumes 0.216 MJ (0.06 kW h) per pressing plus 138.6 MJ (38.5 kWh) during sintering. For 10 presses, the total energy consumed is $((0.06 \times 10)) + 38.5) = 39.1\,kWh$, which is slightly higher than the energy consumed for CSP, demonstrating its edge over TSP.

However, it is immediately clear that from a purely energy consumption perspective, there cross-over point during which the advantages of CSP may become diminished compared to TSP as depicted schematically in Fig. 9. So the key question is 'where does this cross over point lie based on the laboratory scenario described above'? This point can be established by finding the point of equilibrium when $Q_{csp} = Q_{tsp}$. For simplicity sake, let $Q_{csp} = 3.6 \times \left(\frac{m_f}{m_y}\right)$, where m_f = total

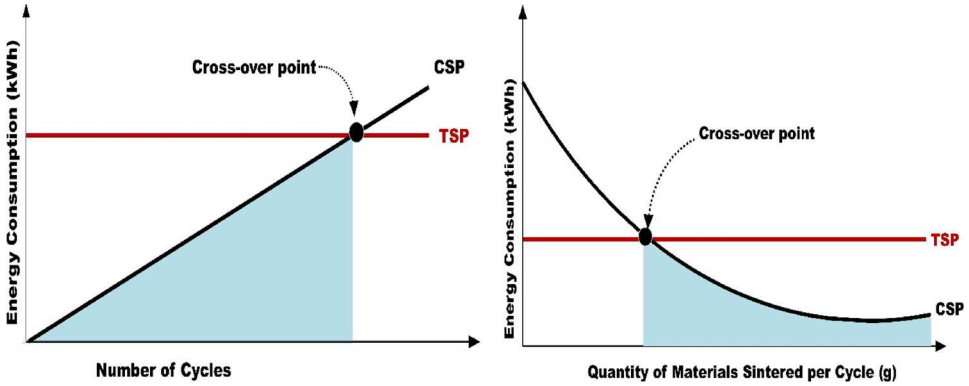

Fig. 9. Schematic representation of cross over point between CSP and traditional or conventional sintering process (TSP), for example, based on representative materials. (a) Cross over point based on number of cycle for complete sintering of materials; (b) Cross over point based on quantity of materials sintered per cycle.

amount of materials to be sintered using CSP; m_y = the maximum allowable amount of materials per unit cycle of CSP (i.e. amount of materials for one press or sintering, which is 100 g per press in this case). Let $N = \frac{m_f}{m_y}$ is the total number of cycles during the entire CSP operation (i.e. total number of presses/sintering throughout the entire operation). On the other hand, $Q_{tsp} = [0.06 \times \left(\frac{m_f}{100}\right) + 38.5]$. Give that m_y is 100 g, by equating Q_{csp} with Q_{tsp}, we have $3.6 \times \left(\frac{m_f}{100}\right) = [0.06 \times \left(\frac{m_f}{m_y}\right) + 38.5]$, from where we solve for m_f which is ˜1088 g and N is ˜ 11. Essentially, 1088 g of ZnO is the maximum allowable quantity to be sintered for CSP (i.e. the cross over point) to maintain its edge in terms of energy consumption. In other words, under the current scenario described, if the total amount of material to be sintered by CSP is > 1088 g, its energy consumption will surpass that of TSP. Put in a different way, if the total number of cycle (i.e. the number of pressing) exceeds 11 cycles, CSP will begin to consume more energy than TSP.

The scenario described above is only valid when the focus is on energy consumption alone. However, looking at energy consumption in isolation is not the optimal way to compare CSP with other techniques given that there are other factors that must be considered to be able to ascertain the overall competitive edge of CSP. In section 4, the framework for a more encompassing figure of merit, which combines other important factors such as initial investment cost of the sintering equipment, cost of energy saved, potential energy and emissions savings is presented. This is premise for the comparison of different sintering techniques considered in this work.

4. Methodology

This section describes the methodology which forms the basis for ranking the cost-effectiveness and energy saving potentials of identified sintering techniques.

4.1. Framework for comparative techno-economic analysis of energy consumption profiles of sintering techniques

In this section, the techno-economic analysis framework based on Marginal Abatement Cost Curve (MACC) and Pareto optimisation is used to compare the effectiveness of each of the sintering techniques based on a standard figure of merit (i.e. cost of per tonne of CO_2 saved or cost per kWh energy saved). A MACC (Fig. 10) provides an illustration of the relationship between the "cost-effectiveness" (i.e. £/tCO_2e) of different sintering techniques and the total amount of energy or CO_2 saved [167,168]. The "cost-effectiveness" for each sintering technique based on different material composition can be calculated using the relation [169]:

$$C_{eff}\ (£/tCO_2) = \frac{\text{Cost of energy saving}(£/kWh)}{CO_2 \text{ savings made } (tCO_2/kWh)} \quad (21)$$

Eq. (21) can also be expressed as [170]:

$$C_{eff} = \frac{\text{Total investment cost } (£) - \text{NPV of the cost of enery saved } (£)}{CO_2 \text{ saved per year } (tCO_2e) \times \text{Number of years}} \quad (22)$$

Moving along the curve (Fig. 10) from left to righ, the "cost-effectiveness, C_{eff}" deteriorates (i.e. each tonne of CO_2e saved becomes costlier) as the total level of emissions reduction increases. On the MACC, different sintering technique occupy different positions. For instance, hypothetical sintering techniques (A and B) which has the capacity to reduce emissions and save money (i.e. the *net present value (NPV) of the cost of energy saved > total investment cost*) are termed negative cost sintering techniques and hypothetical sintering techniques (C to E) that may be responsible for greater reduction in emissions, but incur a positive cost (i.e. *NPV of the cost of energy saved < total investment cost*) are termed positive cost sintering techniques. For detail information on theory of MACC, see Taylor [171] and Ibn-Mohammed et al. [172]. As illustrated in Fig. 10, hypothetical sintering technique A, for example, represents the most economically attractive sintering technique, indicating reduced capital costs and a considerable reduction in CO_2 emissions relative to the baseline sintering energy consumption.

4.1.1. Calculation of the cost of energy saved

The abatement costs of each of the sintering techniques is computed based on overall costs (primarily investment costs) and benefits (energy savings and reductions in CO_2 emission) over a defined time-period. For each sintering technique considered, the following information will be calculated: **(i)** energy saved (kWh) per annum; **(ii)** equivalent CO_2 saved per annum with respect to the base line sintering energy consumption; **(iii)** total investment cost of the equipment and **(iv)** cost of energy (i.e. cost of electricity associated with a sintering technique). The baseline sintering energy consumption is a key element of the entire energy production procedure given that CO_2 savings for each of the sintering techniques is expressed as a percentage of *part* of the baseline. The combination of these data inputs within the TEA framework will lead to the optimal ranking of the effectiveness and efficiencies of each sintering technique with respect to their energy or emissions saving potentials. This will allow us to classify sintering techniques into those that are able to reduce energy consumption and save money and those that may reduce energy consumption but require a net investment. From these datasets, the cost of energy saved (£) per annum is calculated using Eq. (23):

$$\text{Cost of energy saved} = \text{Energy saved (kWh)} \times \text{cost of energy}(£/kWh) \quad (23)$$

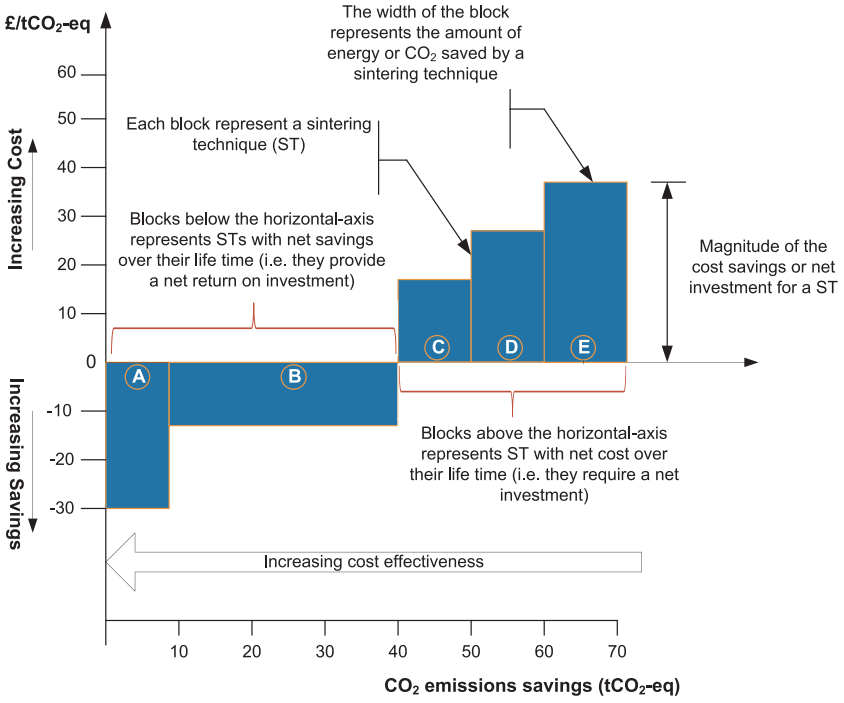

Fig. 10. Illustration of Marginal Abatement Cost Curve for the ranking of sintering techniques based on cost per tonne of CO_2 saved. Note that the use of A, B, C, D and E is to illustrate possible scenarios which do not directly and necessarily relate to a specific existing sintering method. The goal is to introduce the concept to facilitate its understanding and how it is eventually used for the ranking of the specific sintering techniques under consieration.

4.1.2. Net Present Value (NPV) of the cost of energy saved

To evaluate the cost-effectiveness, the concept of Net Present Value (NPV) which measures the profitability derived from adopting a particular sintering technique, must be known. This is computed by discounting the cash flow at the specified rate of return. A positive NPV indicates an investment that returns a profit and a negative NPV suggests that the costs of investments outweighs the expected benefits. The NPV of the cost of energy saved is evaluated by discounting all future savings to their corresponding present value based on the formula [173]:

$$\mathrm{NPV} = \mathrm{C}\left[\frac{1-(1+\mathrm{r})^{-\mathrm{n}}}{\mathrm{r}}\right] \tag{24}$$

Equation (24) represents the net present value, $\boldsymbol{NPV}$, for a yearly energy saving, $\boldsymbol{C}$, occurring for number of years $\boldsymbol{n}$ with a real discount rate of $\boldsymbol{r}$. The main concern with the calculation of NPV is the careful selection of an appropriate discount rate. To calculate NPV, the discount rate must be selected with intuition given that it can pose substantial consequences on the cost-effectiveness of the sintering technique under consideration.

4.1.3. Ranking of negative cost sintering techniques

Although the principle of MACC is a vital tool for ranking the cost-effectiveness of CO_2 abatement options (sintering techniques in this case) based on a standard figure of merit £/tCO_2, a number of studies has however emphasised the discrepancies emanating from its development and interpretation regarding the ranking and prioritisation of measures with negative cost [171,172,174–176]. This is illustrated with an example using the data in Table 1 below.

As indicated in Table 1, it is clear that sintering technique A should typically be the better option because both the economic net benefit and the CO_2 emissions savings are higher in comparison to sintering technique B, for example. However, the standard figure of merit (i.e. £/tCO_2e) based on Eqs. (21) or (22) leads to inaccurate ranking leading to a faulty decision, which prioritises the selection of sintering technique B. This flaw is quite significant because wrong ranking implies a potential failure to realise the optimal result in terms of which sintering technique offers best value for money and CO_2 emission potential.

In this work, the concept of Pareto optimisation [170,171] is employed to mitigate such ranking anomalies when they occur. Although other methods for addressing this flaw within a MAC framework has also been put forward by authors such as Levihn [174] and Ponz-Tienda, Prada-Hernández [175], Pareto optimisation was adopted because it is easier to implement and is more easily comprehended by practitioners as an alternative method of ranking. Pareto optimisation is used when a solution is required in the midst of objectives that are conflicting and where solutions are selected such that there are reasonable trade-offs among different objectives [177]. Within the Pareto optimisation scheme, rather than generating a single optimal solution, solutions are generated that satisfy the criterion of Pareto optimality. Named after Vilfredo Pareto, the principle is such that, if two alternatives $\boldsymbol{x}$ and $\boldsymbol{y}$ are to be ranked, based on a criterion f, such that $\boldsymbol{f_{xi} \geq f_{yi}}$ for all the conditions $(1 \leq \boldsymbol{i} \leq \boldsymbol{p})$, with a minimum of at least one inequality, then it is said that alternative $\boldsymbol{x}$ dominates $\boldsymbol{y}$.

Ranking of negative cost sintering technique is essential to maximise two criteria namely (i) an improved emission or energy saving performance (S), which maps a higher (i.e. more positive) value of S, and (ii) an improved economic gain (N), corresponding to a lesser (i.e. more negative) value of N. Consequently, if say, sintering technique X dominates sintering technique Y then the Pareto expression is written as:

Table 1
Comparison of two sintering technique illustrating a flaw in the calculation formula for cost-effectiveness.

Abatement options	Sintering technique A	Sintering technique B
Net cost of CO_2 emissions saved (£)	−200	−100
CO_2 saved (tCO_2)	20	4
Cost per tonne of CO_2 saved (£/tCO_2)	−10	−25

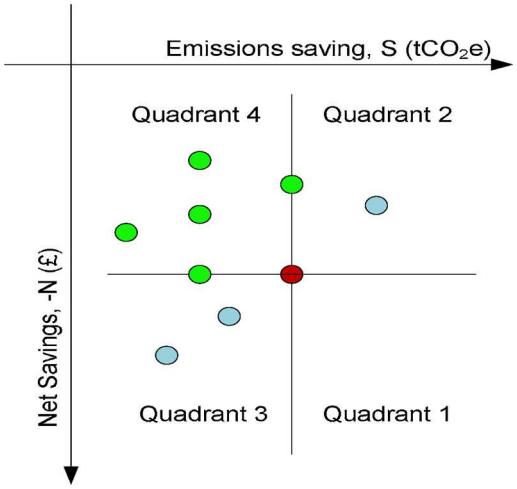

Fig. 11. Ranking of negative cost measure using Pareto optimisation. Adapted from Taylor [171].

$N_X < N_Y$ and $S_X \geq S_Y$, or

$N_X \leq N_Y$ and $S_X > S_Y$

This implies that, if the negative net cost (N) or the emissions saving potential (S) of sintering technique X is better than Y and the other is not worse off. Taylor [171] proposed plotting emissions reduction measures as points on the x–y plane (Fig. 11) with x and y given by the criterion values - emissions saving, S (tCO_2e) and net cost savings, N (£). The points in the Pareto frontier of this initial set are ranked first. These ranked first points are then removed and the points in the Pareto frontier for the remaining set are ranked second. The process is repeated until all the points have been ranked.

4.2. Data sources

The three materials considered in this work and for which data were collected are zinc oxide (ZnO), lead zirconate titanate (PZT) and barium titanate ($BaTiO_3$) given that research on cold sintering processing of these materials have been published. ZnO is a ubiquitous and round-robin material used in many functional devices and can be readily sintered by all the proposed low energy routes. It is an attractive ceramic material which finds a wide range of applications in electrical, optical and medical functions [178,179]. Its non-linear electrical properties renders it an indispensable material for the varistors industries. Due to their excellent electrical properties, PZT piezoelectric ceramics are widely employed in ultrasound transducers, energy harvesters, sensors and precise positioning actuators [161]. Piezoelectric-based devices also act as drivers for enabling technology in a wide array of industries [180]. $BaTiO_3$ is regarded as one of the most vital functional electroceramics and is the basic material for the fabrication of multilayer ceramic capacitor (MLCC) in which several millions of devices are produced each year whilst underpinning the electrical systems in today's world [15].

Data for the duration of sintering operations and manufacturing routes for each materials under different sintering techniques are obtained from published research articles as shown in Table 2. The capital costs and the power ratings of equipment for each of the sintering techniques considered in the analysis are estimated based on current market prices as obtained from https://www.alibaba.com as well as a mix of literature and heuristic information. All cost data were originally quoted in dollars which was converted to the pounds equivalent. As at the time of conducting this analysis, 1 USD amount to 0.7613 GBP. Given that all sintering processes are conducted using electrical equipment in the lab, the corresponding electrical energy consumed (kWh) is computed through the multiplication of the electrical power rating (W) of the sintering equipment as described by the manufacturer and the time (sec) during which the sintering operation is carried out. Cost of electrical energy was taken as 13.3 pence which is the typical rate for non-domestic buildings such as university buildings in the UK, from which the overall cost of energy saved is calculated. Appropriate greenhouse gas emissions factor of 0.5246 $kgCO_2$-eq/kWh was used to convert energy consumption into carbon dioxide equivalent.

5. Results, analysis and discussion

5.1. Indicative percentage CO_2 emissions savings potential of sintering techniques as a function of baseline energy consumption

A range of sintering techniques for processing different ceramic materials considered in this work were analysed in terms of their operational energy and emissions savings potential using the framework described in Section 4.1. All energy consumed during the entire cycle of sintering operation for each of the sintering techniques considered are based on the power rating of the sintering equipment and the duration of the sintering as detailed in Tables 3–5. The energy consumed is then compared with an assumed baseline energy consumption (i.e. the reference energy consumption for a laboratory where different sintering activities are carried out) which is a function of an assumed maximum operating temperature and time, dependent on kit but independent of materials. The difference between the energy consumed during sintering and baseline energy consumption is the energy saved which then constitute the input data into the MACC and Pareto optimisation model for ranking purposes as highlighted in Section 4. The assumed baseline energy consumption for both ZnO and $BaTiO_3$ is 2000 kW h and 3000 kW h for PZT. Tables 3–5 provides an estimation of the energy and indicative CO_2 savings from sintering techniques for processing the materials under consideration. As shown in Table 3, for example, the energy saved during cold sintering of ZnO is 2000 kW h minus 180 kW h which equals 1820 kW h. We assume that 5 kg of each material is sintered based on different number of cycles as indicated in the tables.

The percentage savings of each of the selected sintering technique were evaluated as a function of the baseline CO_2 equivalent emissions for the three materials under consideration is shown in Fig. 12. As indicated, spark plasma sintering and microwave sintering techniques yielded the largest percentage energy and emissions savings for all materials under consideration due to the lower sintering duration (3 min for SPS and 30 min for microwave). For the particular case of cold sintering, it can be observed that for ZnO, the percentage energy or emission savings (91%) is higher compared to the savings attributed to PZT (65%) and $BaTiO_3$ (52%). This striking difference in energy saving potential is attributed to the additional energy required for post annealing process for which both materials (i.e. PZT and $BaTiO_3$) are subjected to in order to establish a thorough crystallisation whilst improving their relative densities [15,161].

As highlighted in Section 3.3, the competitive edge of a sintering technique cannot be determined in absolute terms by looking at energy savings potentials in isolation without considering other factors such as initial capital investment and cost-effectiveness over an extended period of time. In the section that follows, the ranking of the sintering techniques based on the criterion (i.e. the amount of money invested per energy or emissions saved) described in equations 21/22 is presented.

5.2. Comparison of the "cost-effectiveness" of different sintering techniques for materials under consideration

The cost of energy saved is calculated based on Eq. (23). NPV of the energy saved was calculated based on Eq. (24) using a discount rate of 5% over 15 years to allow the flow of cash happening over an extended period to be considered at equivalent value in comparison to energy prices of today. With known values of NPV of the energy saved, the

Table 2
Data sources for the duration of sintering operations and manufacturing routes.

Sintering techniques	ZnO	PZT	$BaTiO_3$
Cold sintering	Funahashi et al. [134,139]	Wang et al. [161]	Guo et al. [15,27,159]
Conventional sintering	Aimable et al. [181]	Ibn-Mohammed et al. [182]	Kim and Han [183]
Spark plasma sintering	Aimable et al. [181]	Wu et al. [184]	Valdez-Nava et al. [151]
Microwave sintering	Zuo et al. [185]	Ramana et al. [186]	Takahashi et al. [57]
Flash sintering	Schmerbauch et al. [187]	Su et al. [188]	M'Peko et al. [189]
Liquid phase sintering	German et al.	Hayashi et al. [190]	Adachi et al. [191]
Hot pressing	Mazaheri [192]	Ewsuk and Messing [193]	Hirata et al. [194]

Table 3
Estimated energy savings from sintering techniques for processing ZnO ceramics.

Sintering techniques	Power rating (W)	Time (s)	Electrical energy consumed per cycle (kWh)	No. of cycle	Total energy consumed (kWh)	Energy saved (kWh)
Cold sintering	1800	7200	3.60	50	180.00	1820.00
Conventional sintering	5500	25200	38.50	10	385.00	1615.00
Spark plasma sintering	50000	300	4.17	10	41.67	1958.33
Microwave sintering	3000	6300	5.25	10	52.50	1947.50
Flash sintering	50000	3300	45.83	20	916.67	1083.33
Liquid phase sintering	12000	7200	24.00	20	480.00	1520.00
Hot pressing	25000	18000	125.00	10	1250.00	750.00

Table 4
Estimated energy from sintering techniques for processing PZT ceramics.

Sintering techniques	Power rating (W)	Time (s)	Electrical energy consumed per cycle (kWh)	No. of cycle	Total energy consumed (kWh)	Energy saved (kWh)
Cold sintering	1800	9000	4.50	50	225.00	2775.00
Cold sintering (annealing)	5500	10800	16.50	50	825.00	2175.00
Conventional sintering	5500	10800	16.50	10	165.00	2835.00
Spark plasma sintering	50000	600	8.33	10	83.33	2916.67
Microwave sintering	3000	1800	1.50	10	15.00	2985.00
Flash sintering	50000	7200	100.00	10	1000.00	2000.00
Liquid phase sintering	12000	7200	24.00	20	480.00	2520.00
Hot pressing	25000	28800	200.00	10	2000.00	1000.00

Table 5
Estimated energy savings from sintering techniques for processing $BaTiO_3$ ceramics.

Sintering techniques	Power rating (W)	Time (s)	Electrical energy consumed per cycle (kWh)	No. of cycle	Total energy consumed (kWh)	Energy saved (kWh)
Cold sintering	1800	5400	2.70	50	135.00	1865.00
Cold sintering (annealing)	5500	10800	16.50	50	825.00	1175.00
Conventional sintering	5500	18000	27.50	10	275.00	1725.00
Spark plasma sintering	50000	180	2.50	10	25.00	1975.00
Microwave sintering	3000	1800	1.50	10	15.00	1985.00
Flash sintering	50000	900	12.50	10	125.00	1875.00
Liquid phase sintering	12000	7200	24.00	20	480.00	1520.00
Hot pressing	25000	12000	83.33	10	833.33	1166.67

total cost of each sintering technique and the corresponding energy or emissions savings, the cost-effectiveness of each sintering technique for the fabrication of the materials under consideration are the calculated as shown in the subsections that follows.

5.2.1. The case of ZnO

Table 6 shows the calculated values towards the ranking of the "cost-effectiveness" of different sintering techniques for processing ZnO and the resulting ranking within a MACC framework is depicted in Fig. 13. As shown, only cold sintering of ZnO resulted in a win-win situation where there is a return on investment -£989.83 with a corresponding CO_2 emissions savings of 14.32 tCO_2-eq. As shown in Fig. 13, although sintering technique such as spark plasma sintering saved more CO_2 emissions (15.41 tCO_2-eq), it comes at a cost which is attributed to the expensive nature of the SPS equipment. The use of ranking principle based on Pareto optimisation is not applied here given that CSP is the only sintering technique that resulted in a negative cost. Overall, CSP is the most economically attractive sintering option, indicating lower capital costs and best return on investment as well as considerable energy and emission savings for the processing of ZnO ceramic materials.

5.2.2. The case of PZT

Table 7 and Fig. 14 shows the ranking of sintering techniques for processing PZT ceramic. As indicated, CSP and conventional sintering are negative cost sintering techniques. Although the conventional sintering saves more CO_2 emissions (22.31 tCO_2-eq) compared to CSP (15.34 tCO_2-eq), however, CSP offers an improved economic gain (-£1169.29) compared to -£487.86 for conventional sintering, hence the ranking of CSP ahead of conventional sintering in terms of return on

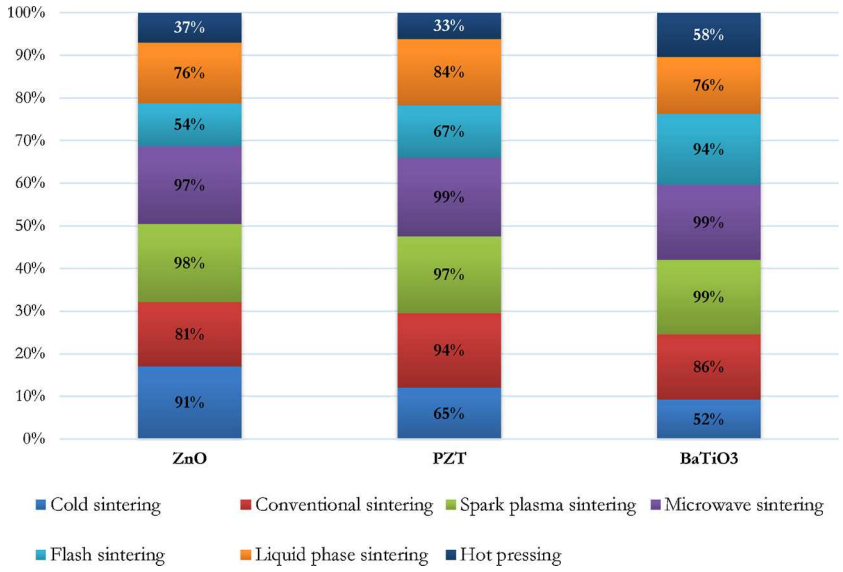

Fig. 12. Indicative CO_2 savings from sintering techniques as a function of percentage reduction in baseline energy consumption.

investment, based on Pareto ranking. Again, CSP is the most economically attractive sintering option, due to its lower capital costs and huge return on investment with considerable energy and emission savings for the processing of PZT ceramic materials.

5.2.3. The case of $BaTiO_3$

For the case of $BaTiO_3$, the ranking of the cost effectiveness of the sintering techniques are depicted in Fig. 15 based on Table 8 indicating for the first time an instance where CSP becomes a positive cost sintering technique but still offer the most cost-effective technique in comparison to others. The reason for this is that as shown in Tables 4 and 5, cold sintering time (9000 s) for PZT ceramic is greater than that for $BaTiO_3$ ceramics (5400 s) but the time for annealing for both materials is the same. So the total energy consumed for PZT is 1050 kW h (i.e. 225 + 825) and 960 kW h (i.e. 135 + 825), for $BaTiO_3$. However, the assumed baseline energy consumption for PZT is 3000 kW h and 2000 kW h for $BaTiO_3$. Baseline for PZT is chosen to be higher given that energy saved by other sintering techniques are significantly higher than 2000 kW h (see Table 4), so that the overall energy saved and by extension the cost of energy saved for $BaTiO_3$ ceramic (£138.32) is lower than for PZT (£259.35). Accordingly, the NPV of energy saved of $BaTiO_3$ ceramic is lower than the capital cost of the CSP equipment, hence its profile as a positive cost sintering technique in this case. Overall, CSP still constitute the most economically attractive sintering option, indicating lower capital costs and best return on investment as well as considerable energy and emission savings for the processing of $BaTiO_3$ ceramic material.

5.3. Sensitivity analysis: effect of change in discount rate

A time frame of 15 years was adopted to allow for net present value calculations. The number of years can be chosen at the discretion of the analyst and it does not affect the results. The use of a discount rate of 5% is in line with standard practice in investment appraisal analysis. Generally speaking, two approaches namely prescriptive approach (or social perspective) and descriptive approach (or industry perspective) are used to guide the choice of the discount factor [195]. The prescriptive approach is mainly employed for long-term issues such as energy efficiency, environmental pollution or public sector projects and uses lower discount rates of between 4 and 10% [195]. The use of low discount rates present the advantage of treating future generations equally. On the other hand, the descriptive approach uses relatively high discount rates of 10–30% with the aim of reflecting the existence of barriers to energy efficiency investments, for example [195].

Indeed, results of the overall energy saving performance of a sintering options can vary from study to study depending on several variables such as the costs of electricity and sintering equipment as well as the choice of discount rate. In particular, the choice of discount rate can influence results of the overall cost-effectiveness of the sintering techniques considered but it does not alter the ranking or the decision making because all options are analysed using the same discount rate. In this paper, a discount rate of 5% is used throughout. Table 9 presents

Table 6
Ranking of sintering techniques for processing ZnO ceramic.

Sintering techniques	Capital cost (£), C	Cost of energy saved (£)	NPV of energy saved (£), E	Net savings or Net Cost (£), N [C-E]	tCO_2e saved across 15 years, S	Cumulative savings (tCO_2e)	£/tCO_2 saved, M [N/S]	Ranking
			Negative cost sintering techniques					**Pareto**
Cold sintering	1522.67	242.06	2512.50	−989.83	14.32	14.32	N/A	1
			Positive cost sintering techniques					**MAC**
Conventional sintering	3425.84	94.14	977.12	1196.34	12.71	27.03	94.14	2
Microwave sintering	4811.39	142.81	2688.51	2122.88	15.32	42.35	138.52	3
Liquid phase sintering	3806.48	717.61	2098.35	1708.13	11.96	54.32	142.81	4
Hot pressing	4567.8	2294.68	1035.37	3532.43	5.90	60.22	598.54	5
Flash sintering	7612.97	598.54	1495.53	6117.44	8.52	68.74	717.61	6
Spark plasma sintering	38064.85	138.52	2703.47	35361.38	15.41	84.15	2294.68	7

Not applicable (NA): implies that for negative cost sintering technique Pareto Optimisation was used for the ranking but its importance is not demonstrated because only one option (CSP) falls under negative cost and therefore represents the most economically attractive option.

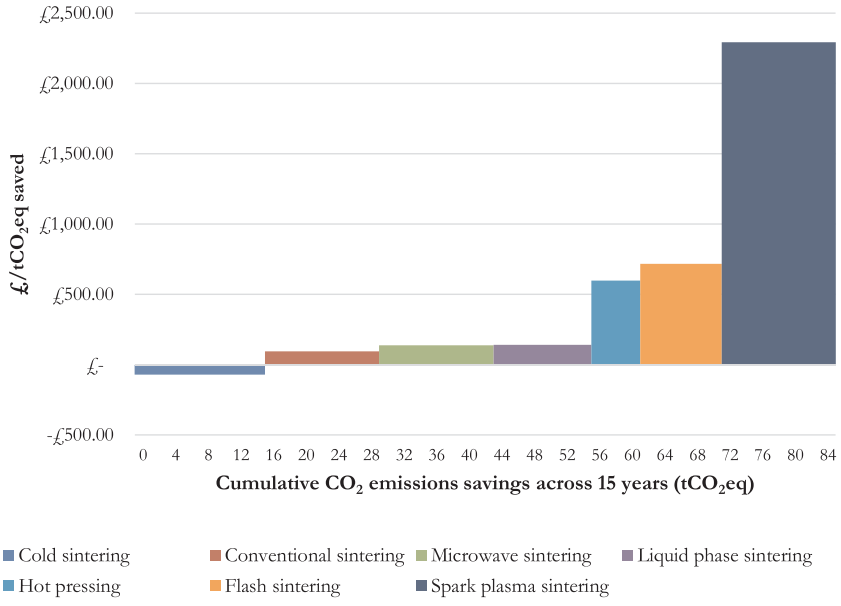

Fig. 13. Ranking of cost-effectiveness of sintering techniques for ZnO ceramic.

the results of sensitivity analysis, showing how changes in the discount rate influence the cost-effectiveness of the sintering techniques under consideration, using the case of ZnO, for example. As shown, an increase in discount factor leads to an increase in the net present value of energy saved, net savings and consequently the cost-effectiveness (£/tCO_2-eq) but the overall ranking of the sintering techniques remains the same, with CSP still coming up as the most cost-effective under the scenarios considered within a laboratory setting.

6. Study limitation

Despite the results reported, we note that the analysis suffers from a number of limitations:

i The choice of baseline energy consumption within the laboratory could be established in a more rigorous way by defining boundaries (i.e. load distribution across the laboratory) and gathering energy use data.
ii The cost of CSP used in the calculation is based on current infrastructure in the laboratory and does not include the assembling time costs, cost of machinery to automate a full line with CSP to attain industrial level production rates. These costs implications are difficult to predict at the moment and are therefore beyond the scope of the current work. However, all sintering techniques were considered at the laboratory levels.
iii The number of cycles of sintering were also based on assumptions due to difficulty in predicting them accurately. Changes to the number of cycles per sintering operation may affect the cost-effectiveness of the techniques under consideration.
iv The mathematical model presented assumes perfect insulation of the sintering chamber and a negligible heat loss. Furthermore, it is assumed that the properties of the powder compact being sintered in all processes are similar. The effect of sintering-enhancing pretreatment of the powder compact is neglected.

7. Conclusion and summary

On a global level, the industrial sector is a vibrant source of wealth, affluence and social value given its responsibility for roughly one-quarter of global GDP and employment, whilst producing materials and commodities that are essential to our daily lives. One of the energy intensive industrial sectors that has the potential to improve efficiency by leveraging modern energy reduction technologies is the ceramic sub-sector. As such, it has been identified as one of the key sub-sector within the industrial sector targeted for energy reduction. Ceramics generally vary from technical (heat or impact resistant), electronics (capacitors, insulators, Li-ion batteries, and microwave devices), architectural and white wares with a wide range of applications that plays key roles in the society by enabling resource and energy efficiency in other sectors.

A key process within the ceramic sector which is responsible for high energy consumption is the sintering. Densification at very high temperatures of up to 1800 °C results in the emission of GHGs and high energy costs. High processing temperatures also restrict compatibility of ceramics with polymers or metals and hinders the development of

Table 7
Ranking of sintering techniques for processing PZT ceramic.

Sintering techniques	Capital cost (£), C	Cost of energy saved (£)	NPV of energy saved (£), E	Net savings or Net Cost (£), N [C-E]	tCO_2e saved over 15 years, S	Cumulative savings (tCO_2e)	£/tCO_2 saved, M [N/S]	Ranking
			Negative cost sintering techniques					**Pareto**
Cold sintering	1522.67	259.35	2691.96	−1169.29	15.34	15.34	N/A	1
Conventional sintering	3425.84	377.05	3913.70	−487.86	22.31	37.65	N/A	2
			Positive sintering techniques					**MAC**
Microwave sintering	4811.39	397.00	4120.78	690.61	19.83	57.48	16.52	3
Liquid phase sintering	3806.48	335.16	3478.85	327.63	23.49	80.97	29.40	4
Hot pressing	4567.8	133.00	1380.49	3187.31	15.74	96.71	308.30	5
Flash sintering	7612.97	266.00	2760.99	4851.98	7.87	104.58	405.05	6
Spark plasma sintering	38064.85	387.92	4026.44	34038.41	22.95	127.53	1483.07	7

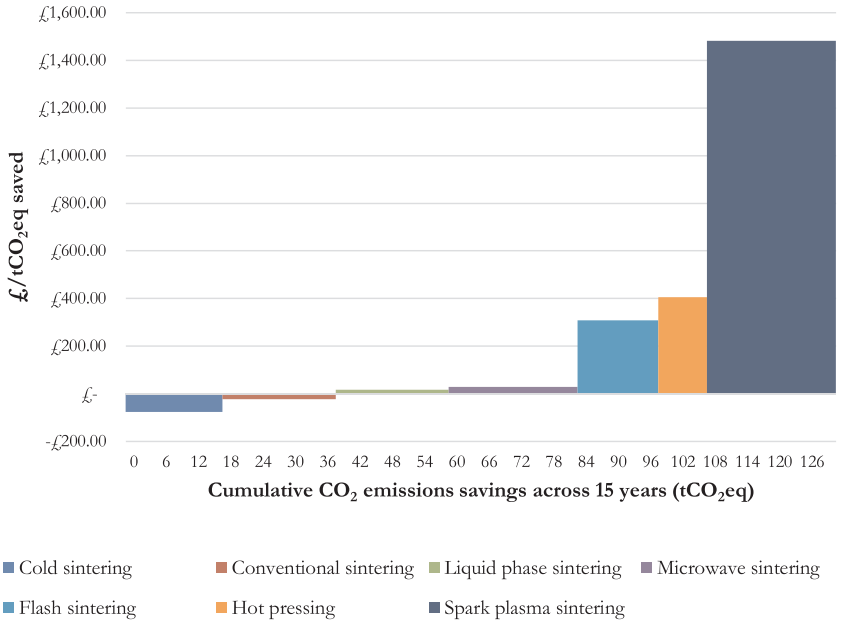

Fig. 14. Ranking of cost-effectiveness of sintering techniques for PZT ceramic.

ceramic/ceramic composite technology. The challenge therefore is for the sector to explore and apply new technologies to reduce energy consumption and this has prompted global-wide research in scientific communities and industrial setting towards the development of numerous sintering theories and innovations.

Recent results have demonstrated that manufacturing of ceramics can be achieved at much lower temperatures (100–150 °C) under modest pressures using a modified hydrothermal process termed Cold Sintering Process. This radical, low temperature approach relies on the formation or the use of aqueous salts which permit a combination of particle rearrangement (compaction) followed by the precipitation of the matrix phase on the surface of the crystallite. Despite the research success achieved in developing low temperature sintering process, the viability of cold sintering as a competitive and sustainable alternative to other traditional high temperature ceramic manufacturing techniques is not established. Thus, we present a rigorous comparative techno-economic analysis of a number of sintering techniques, based on the ranking principles of marginal abatement cost curve (MACC) and Pareto optimisation. In doing so, we classified sintering techniques into those that are able to reduce energy consumption and save money and those that may reduce energy consumption but requiring a net investment.

By using pounds per tonne of CO_2 saved as a figure of merit to measure the cost-effectiveness of each sintering technique at the level of the laboratory, it was established that CSP is the most economically attractive sintering technique, indicating lower capital costs, best return on investment and a considerable reduction in CO_2 emissions for the processing of three ceramic materials namely ZnO, PZT and $BaTiO_3$, even under projected mass production scenarios. However, for CSP to realise its full potential and transition from laboratory to industry, several conditions must be met, including: (i) understanding the significance of a number of factors such as grain size and morphology, particle size distribution, die sealing, rate of pressure application, and liquid phase viscosity; (ii) development of a generalised and unified

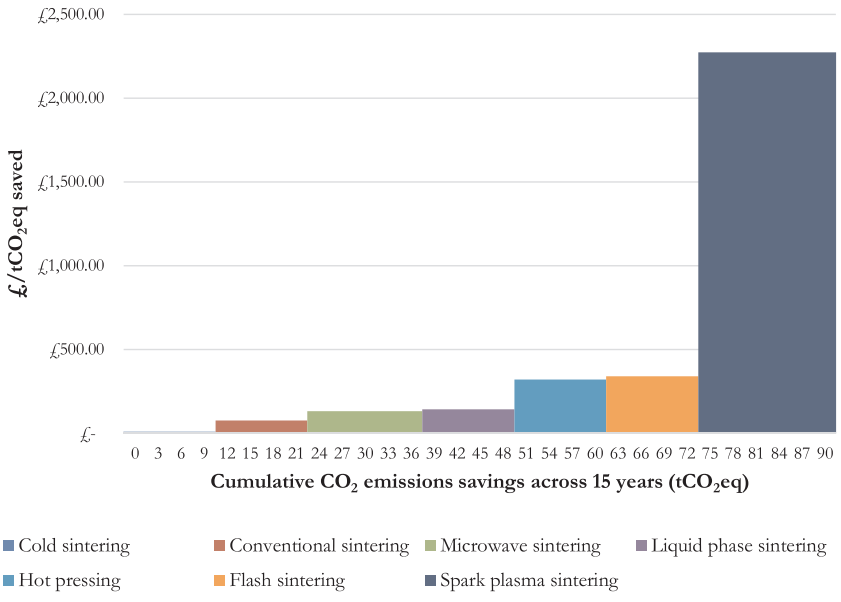

Fig. 15. Ranking of cost-effectiveness of sintering techniques for $BaTiO_3$ ceramic.

Table 8
Ranking of sintering techniques for processing $BaTiO_3$ ceramic.

Sintering techniques	Capital cost (£), C	Cost of energy saved (£)	NPV of energy saved (£), E	Net savings or Net Cost (£), N [C-E]	tCO_2e saved over 15 years, S	Cumulative savings (tCO_2e)	£/tCO_2 saved, M [N/S]	Ranking
Positive sintering techniques								**MAC**
Cold sintering	1522.67	138.32	1435.71	86.96	8.18	8.18	10.63	1
Conventional sintering	3425.84	229.42	2381.35	1044.49	13.57	21.76	76.95	2
Microwave sintering	4811.39	264.00	2740.28	2071.11	15.62	37.38	132.59	3
Liquid phase sintering	3806.48	202.16	2098.35	1708.13	11.96	49.34	142.81	4
Hot pressing	4567.8	155.17	1610.58	2957.22	9.18	58.52	322.12	5
Flash sintering	7612.97	249.37	2588.43	5024.54	14.75	73.27	340.55	6
Spark plasma sintering	38064.85	262.67	2726.48	35338.37	15.54	88.81	2273.84	7

Table 9
Sensitivity analysis on the effect of change in discount rate.

Sintering technique	NPV of energy saved (£)	Net savings (£)	£/tCO_2 saved
5% discount rate			
Cold sintering	2512.50	−989.83	−69.11
Conventional sintering	2229.50	1196.34	94.14
Microwave sintering	2688.51	2122.88	138.52
Liquid phase sintering	2098.35	1708.13	142.81
Hot pressing	1035.37	3532.43	598.54
Flash sintering	1495.53	6117.44	717.61
Spark plasma sintering	2703.47	35361.38	2294.68
7% discount rate			
Cold sintering	2204.66	−681.99	−47.62
Conventional sintering	1956.33	1469.51	115.63
Microwave sintering	2359.11	2452.28	160.02
Liquid phase sintering	1841.26	1965.22	164.30
Hot pressing	908.51	3659.29	620.04
Flash sintering	1312.30	6300.67	739.10
Spark plasma sintering	2372.23	35692.62	2316.18
10% discount rate			
Cold sintering	1841.13	−318.46	−22.24
Conventional sintering	1633.75	1792.09	141.02
Microwave sintering	1970.11	2841.28	185.40
Liquid phase sintering	1537.64	2268.84	189.69
Hot pressing	758.71	3809.09	645.42
Flash sintering	1095.91	6517.06	764.49
Spark plasma sintering	1981.07	36083.78	2341.56

CSP framework which can be applied to numerous compositions; (iii) an improvement in the quantity of materials that can be sintered in a single CSP operation; (iv) robust facilities and instrumentation strategy which enhance performance; (v) validations of statistically relevant property and key performance indicators; and (vi) an understanding of the assembling time costs, cost of machinery to automate a full line with CSP, to attain industrial level production rates.

Author contributions

R.I.M, R.C.A, S.D.C. and K.S.C.L, conceived the reseaarch. I-MT and M.K.B developed the mathematical model and methodological notes. I-MT prepared the data with contributions from M.K.B. I-MT, MKB, GJ, WJ, BS conducted the review on the different types of sintering technologies considered. I-MT conducted the analysis of the data and prepared the figures. I-MT, MKB, GJ, WJ, BS and WD wrote the paper with feedback from R.I.M, R.C.A, S.D.C. and K.S.C.L

Declaration of Competing Interest

There are no conflict of interest to declare.

Acknowledgement

This work was financially supported by the Engineering and Physical Sciences Research Council (EPSRC-EP/L017563/1), United Kingdom, through The University of Sheffield, under the project titled: Substitution and Sustainability in Functional Materials and Devices.

References

[1] IPCC, Contribution of Working Group III to the Fifth Assessment Report of the Intergovernmental Panel on Climate Change, (2014).
[2] World Resources Institute, World Greenhouse Gas Emissions in 2005, (2005).
[3] International Energy Agency, CO2 Emissions from Fuel Combustion, (2017).
[4] S. Koh, T. Ibn-Mohammed, A. Acquaye, K. Feng, I. Reaney, K. Hubacek, et al., Drivers of US toxicological footprints trajectory 1998–2013, Sci. Rep. 6 (2016) 39514.
[5] F. Pusavec, P. Krajnik, J. Kopac, Transitioning to sustainable production–part I: application on machining technologies, J. Clean. Prod. 18 (2010) 174–184.
[6] V. Jegatheesan, J. Liow, L. Shu, S. Kim, C. Visvanathan, The need for global co-ordination in sustainable development, J. Clean. Prod. 17 (2009) 637–643.
[7] J.M. Allwood, J.M. Cullen, R.L. Milford, Options for Achieving a 50% Cut in Industrial Carbon Emissions by 2050, ACS Publications, 2010.
[8] R.L. Milford, S. Pauliuk, J.M. Allwood, D.B. Müller, The roles of energy and material efficiency in meeting steel industry CO2 targets, Environ. Sci. Technol. 47 (2013) 3455–3462.
[9] C. Agrafiotis, T. Tsoutsos, Energy saving technologies in the European ceramic sector: a systematic review, Appl. Therm. Eng. 21 (2001) 1231–1249.
[10] Dept. of Business Innovation and Skills, Industrial Decarbonisation and Energy Efficiency Roadmaps to 2050- Ceramics- Pathways to Decarbonisation in 2050, (2015).
[11] The European Ceramic Industry Association, Paving the Way to 2050: the Ceramic Industry Road Map, (2012).
[12] Tangram Technology Ltd, Energy Efficiency in Ceramics Processing: Practical Worksheets for Industry, (2012).
[13] United Nations Industrial Development Organization (UNIDO), Handy Manual of Ceramic Industry. Output of a Seminar on Energy Conservation in Ceramic Industry, (1994).
[14] European Commission, Reference Document on Best Available Techniques in the Ceramic Manufacturing Industry, (2007).
[15] H. Guo, J. Guo, A. Baker, C.A. Randall, Hydrothermal-assisted cold sintering process: a new guidance for low-temperature ceramic sintering, ACS Appl. Mater. Interfaces 8 (2016) 20909–20915.
[16] J. Guo, S.S. Berbano, H. Guo, A.L. Baker, M.T. Lanagan, C.A. Randall, Cold sintering process of composites: bridging the processing temperature gap of ceramic and polymer materials, Adv. Funct. Mater. 26 (2016) 7115–7121.
[17] J. Guo, H. Guo, A.L. Baker, M.T. Lanagan, E.R. Kupp, G.L. Messing, et al., Cold sintering: a paradigm shift for processing and integration of ceramics, Angew. Chemie 128 (2016) 11629–11633.
[18] A. Baker, H. Guo, J. Guo, C. Randall, Utilizing the cold sintering process for flexible–Printable electroceramic device fabrication, J. Am. Ceram. Soc. 99 (2016) 3202–3204.
[19] R. German, Sintering: From Empirical Observations to Scientific Principles, Butterworth-Heinemann, 2014.
[20] E. Gutmanas, A. Rabinkin, M. Roitberg, Cold sintering under high pressure, Scr. Metall. 13 (1979) 11–15.
[21] European Commission, Reference Document on Best Available Techniques in the Ceramic Manufacturing Industry, Available at Integrated Pollution Prevention and Control (IPPC), 2007, http://eippcb.jrc.es.
[22] K.A. Khalil, Advanced Sintering of Nano-Ceramic Materials. Ceramic Materials-progress in Modern Ceramics, InTech, 2012.
[23] M.N. Rahaman, Sintering of Ceramics, CRC press, 2007.
[24] M. Shukla, S. Ghosh, N. Dandapat, A.K. Mandal, V.K. Balla, Comparative study on conventional sintering with microwave sintering and vacuum sintering of Y2O3-Al2O3-ZrO2 ceramics, J. Mater. Sci. Chem. Eng. 4 (2016) 71.
[25] Y. Gu, K. Khor, P. Cheang, Bone-like apatite layer formation on hydroxyapatite

prepared by spark plasma sintering (SPS), Biomaterials 25 (2004) 4127–4134.
[26] C. Tang, P. Uskokovic, C. Tsui, D. Veljovic, R. Petrovic, D. Janackovic, Influence of microstructure and phase composition on the nanoindentation characterization of bioceramic materials based on hydroxyapatite, Ceram. Int. 35 (2009) 2171–2178.
[27] H. Guo, A. Baker, J. Guo, C.A. Randall, Cold sintering process: a novel technique for low-temperature ceramic processing of ferroelectrics, J. Am. Ceram. Soc. 99 (2016) 3489–3507.
[28] J. Rödel, W. Jo, K.T. Seifert, E.M. Anton, T. Granzow, D. Damjanovic, Perspective on the development of lead-free piezoceramics, J. Am. Ceram. Soc. 92 (2009) 1153–1177.
[29] J. Wu, D. Xiao, J. Zhu, Potassium–sodium niobate lead-free piezoelectric materials: past, present, and future of phase boundaries, Chem. Rev. 115 (2015) 2559–2595.
[30] L. Gao, H. Guo, S. Zhang, C.A. Randall, Base Metal Co-Fired Multilayer Piezoelectrics, Actuators: Multidisciplinary Digital Publishing Institute, 2016, p. 8.
[31] G. Yang, S. Lee, Z. Liu, C. Anthony, E. Dickey, Z. Liu, et al., Effect of local oxygen activity on Ni–BaTiO3 interfacial reactions, Acta Mater. 54 (2006) 3513–3523.
[32] H. Shimizu, K. Kobayashi, Y. Mizuno, C.A. Randall, Advantages of low partial pressure of oxygen processing of alkali niobate: NaNbO3, J. Am. Ceram. Soc. 97 (2014) 1791–1796.
[33] N.J. Donnelly, C.A. Randall, Mixed conduction and chemical diffusion in a Pb (Zr 0.53, Ti 0.47) O 3 buried capacitor structure, Appl. Phys. Lett. 96 (2010) 052906.
[34] R. Halouani, D. Bernache-Assolant, E. Champion, A. Ababou, Microstructure and related mechanical properties of hot pressed hydroxyapatite ceramics, J. Mater. Sci. Mater. Med. 5 (1994) 563–568.
[35] D. Veljović, B. Jokić, R. Petrović, E. Palcevskis, A. Dindune, I. Mihailescu, et al., Processing of dense nanostructured HAP ceramics by sintering and hot pressing, Ceram. Int. 35 (2009) 1407–1413.
[36] R.K. Bordia, S.J.L. Kang, E.A. Olevsky, Current understanding and future research directions at the onset of the next century of sintering science and technology, J. Am. Ceram. Soc. (2017).
[37] J.M. Osepchuk, Microwave power applications, IEEE Trans. Microw. Theory Tech. 50 (2002) 975–985.
[38] E.T. Thostenson, T.W. Chou, Microwave processing: fundamentals and applications, Compos. Part A Appl. Sci. Manuf. 30 (1999) 1055–1071.
[39] R.J. Lauf, D.W. Bible, A.C. Johnson, C.A. Everleigh, Two to 18 GHz broadband microwave heating systems, Microw. J. 36 (1993) 24–30.
[40] N.R. Council, Microwave Processing of Materials, National Academies Press, 1994.
[41] D.K. Agrawal, Microwave processing of ceramics, Curr. Opin. Solid State Mater. Sci. 3 (1998) 480–485.
[42] W.H. Sutton, Microwave processing of ceramics - an overview, MRS Proceedings 269 (2011) 3.
[43] H.K. Solanki, V.D. Prajapati, G.K. Jani, Microwave technology—a potential tool in pharmaceutical science, ChemInform 42 (2011) no.
[44] S. Singh, D. Gupta, V. Jain, Recent applications of microwaves in materials joining and surface coatings, Proc. Inst. Mech. Eng. Part B J. Eng. Manuf. 230 (2016) 603–617.
[45] A. Kumar, V.G. Jain, D.G. Gupta, Microwave Joining of Stainless Steel and Their Characterizations, (2015).
[46] P.F. Mead, A. Ramamoorthy, S. Pal, Investigation of variable frequency microwave processing for electronic packaging applications, J. Electron. Packag. 125 (2003) 294–301.
[47] L. Zong, S. Zhou, N. Sgriccia, M. Hawley, L. Kempel, A review of microwave-assist polymer chemistry (MAPC), J. Microw. Power Electromagn. Energy 38 (2003) 49–74.
[48] A. Diaz-Ortiz, A. Moreno, Activation of organic reactions by microwaves, Adv. Org. Synth. 1 (2005) 119–171.
[49] R.M. German, Powder Metallurgy and Particulate Materials Processing: the Processes, Materials, Products, Properties, and Applications: Metal Powder Industries Federation Princeton, (2005).
[50] M. Oghbaei, O. Mirzaee, Microwave versus conventional sintering: a review of fundamentals, advantages and applications, J. Alloys. Compd. 494 (2010) 175–189.
[51] R. Roy, D. Agrawal, J. Cheng, S. Gedevanishvili, Full sintering of powdered-metal bodies in a microwave field, Nature 399 (1999) 668.
[52] M. Gupta, W.L.E. Wong, Enhancing overall mechanical performance of metallic materials using two-directional microwave assisted rapid sintering, Scr. Mater. 52 (2005) 479–483.
[53] K. Rao, P. Ramesh, Use of microwaves for the synthesis and processing of materials, Bull. Mater. Sci. 18 (1995) 447–465.
[54] J. Sun, W. Wang, Q. Yue, Review on microwave-matter interaction fundamentals and efficient microwave-associated heating strategies, Materials 9 (2016) 231.
[55] I. Bilecka, P. Elser, M. Niederberger, Kinetic and thermodynamic aspects in the microwave-assisted synthesis of ZnO nanoparticles in benzyl alcohol, ACS Nano 3 (2009) 467–477.
[56] A. Dorner-Reisel, S. Schöps, A. Lenk, G. Schmutzler, Microstructural comparison of conventional and microwave sintered BaTiO3, Adv. Eng. Mater. 9 (2007) 400–405.
[57] H. Takahashi, Y. Numamoto, J. Tani, K. Matsuta, J. Qiu, S. Tsurekawa, Lead-free barium titanate ceramics with large piezoelectric constant fabricated by microwave sintering, J. Appl. Phys. 45 (2005) L30.
[58] C.-S. Chen, C.-C. Chou, W.-C. Yang, I.-N. Lin, Microwave sintering of base-metal-electroded BaTiO 3 capacitor materials Co-doped with MgO/Y 2 O 3 additives, J. Electroceramics 13 (2004) 573–577.
[59] X.H. Zhu, Q.M. Hang, Microscopical and physical characterization of microwave and microwave-hydrothermal synthesis products, Micron 44 (2013) 21–44.
[60] R.R. Mishra, A.K. Sharma, A review of research trends in microwave processing of metal-based materials and opportunities in microwave metal casting, Crit. Rev. Solid State Mater. Sci. 41 (2016) 217–255.
[61] R.R. Mishra, A.K. Sharma, Microwave–material interaction phenomena: heating mechanisms, challenges and opportunities in material processing, Compos. Part A Appl. Sci. Manuf. 81 (2016) 78–97.
[62] W. Liu, F. Xu, Y. Li, X. Hu, B. Dong, Y. Xiao, Discussion on microwave-matter interaction mechanisms by in situ observation of “core-shell” microstructure during microwave sintering, Materials 9 (2016) 120.
[63] J.D. Katz, Microwave sintering of ceramics, Ann. Rev. Mater. Sci. 22 (1992) 153–170.
[64] M. Vollmer, Physics of the microwave oven, Phys. Educ. 39 (2004) 74.
[65] R. Roy, D. Agrawal, J. Cheng, S. Gedevanishvili, Full sintering of powdered-metal bodies in a microwave field, Nature 399 (1999) 668.
[66] D. Agrawal, Latest global developments in microwave materials processing, Mater. Res. Innov. 14 (2010) 3–8.
[67] M. Omori, Sintering, consolidation, reaction and crystal growth by the spark plasma system (SPS), Mater. Sci. Eng. A 287 (2000) 183–188.
[68] O. Guillon, J. Gonzalez-Julian, B. Dargatz, T. Kessel, G. Schierning, J. Räthel, et al., Field-assisted sintering technology/spark plasma sintering: mechanisms, materials, and technology developments, Adv. Eng. Mater. 16 (2014) 830–849.
[69] M.W. Gaultois, Design Principles for Oxide Thermoelectric Materials, University of California, Santa Barbara, 2015.
[70] B. McWilliams, A. Zavaliangos, Multi-phenomena simulation of electric field assisted sintering, J. Mater. Sci. 43 (2008) 5031–5035.
[71] D. Schwesig, G. Schierning, R. Theissmann, N. Stein, N. Petermann, H. Wiggers, et al., From nanoparticles to nanocrystalline bulk: percolation effects in field assisted sintering of silicon nanoparticles, Nanotechnology 22 (2011) 135601.
[72] A. Becker, S. Angst, A. Schmitz, M. Engenhorst, J. Stoetzel, D. Gautam, et al., The effect of Peltier heat during current activated densification, Appl. Phys. Lett. 101 (2012) 013113.
[73] M. Beekman, M. Baitinger, H. Borrmann, W. Schnelle, K. Meier, G.S. Nolas, et al., Preparation and crystal growth of Na24Si136, J. Am. Chem. Soc. 131 (2009) 9642–9643.
[74] Z. Munir, U. Anselmi-Tamburini, M. Ohyanagi, The effect of electric field and pressure on the synthesis and consolidation of materials: a review of the spark plasma sintering method, J. Mater. Sci. 41 (2006) 763–777.
[75] H. Borodianska, L. Krushinskaya, G. Makarenko, Y. Sakka, I. Uvarova, O. Vasylkiv, Si3N4–TiN nanocomposite by nitration of TiSi2 and consolidation by hot pressing and spark plasma sintering, J. Nanosci. Nanotechnol. 9 (2009) 6381–6389.
[76] H. Borodianska, O. Vasylkiv, Y. Sakka, Nanoreactor engineering and spark plasma sintering of Gd20Ce80O1. 90 nanopowders, J. Nanosci. Nanotechnol. 8 (2008) 3077–3084.
[77] O. Vasylkiv, H. Borodianska, Y. Sakka, Nanoreactor engineering and SPS densification of multimetal oxide ceramic nanopowders, J. Eur. Ceram. Soc. 28 (2008) 919–927.
[78] J.G. Santanach, C. Estournès, A. Weibel, A. Peigney, G. Chevallier, C. Laurent, Spark plasma sintering as a reactive sintering tool for the preparation of surface-tailored Fe–FeAl2O4–Al2O3 nanocomposites, Scr. Mater. 60 (2009) 195–198.
[79] R. Licheri, R. Orrù, C. Musa, G. Cao, Combination of SHS and SPS Techniques for fabrication of fully dense ZrB2-ZrC-SiC composites, Mater. Lett. 62 (2008) 432–435.
[80] J. Zhang, L. Wang, L. Shi, W. Jiang, L. Chen, Rapid fabrication of Ti3SiC2–SiC nanocomposite using the spark plasma sintering-reactive synthesis (SPS-RS) method, Scr. Mater. 56 (2007) 241–244.
[81] W.-W. Wu, G.-J. Zhang, Y.-M. Kan, P.-L. Wang, K. Vanmeensel, J. Vleugels, et al., Synthesis and microstructural features of ZrB2–SiC-based composites by reactive spark plasma sintering and reactive hot pressing, Scr. Mater. 57 (2007) 317–320.
[82] O. Vasylkiv, H. Borodianska, P. Badica, Y. Zhen, A. Tok, Nanoblast synthesis and consolidation of (La0. 8Sr0. 2)(Ga0. 9Mg0. 1) O3–σ under spark plasma sintering conditions, J. Nanosci. Nanotechnol. 9 (2009) 141–149.
[83] K. Morita, B.-N. Kim, K. Hiraga, H. Yoshida, Fabrication of transparent MgAl2O4 spinel polycrystal by spark plasma sintering processing, Scr. Mater. 58 (2008) 1114–1117.
[84] J.-K. Park, U.-J. Chung, D.-Y. Kim, Application of spark plasma sintering for growing dense Pb (Mg 1/3 Nb 2/3) O 3–35 mol% PbTiO 3 single crystal by solid-state crystal growth, J. Electroceramics 17 (2006) 509–513.
[85] C. Elissalde, M. Maglione, C. Estournes, Tailoring dielectric properties of multilayer composites using spark plasma sintering, J. Am. Ceram. Soc. 90 (2007) 973–976.
[86] W. Liu, M. Naka, In situ joining of dissimilar nanocrystalline materials by spark plasma sintering, Scr. Mater. 48 (2003) 1225–1230.
[87] Y.J. Wu, N. Uekawa, K. Kakegawa, Sandwiched BaNd2Ti4O12/Bi4Ti3O12/BaNd2Ti4O12 ceramics prepared by spark plasma sintering, Mater. Lett. 57 (2003) 4088–4092.
[88] R. Chaim, R. Marder-Jaeckel, J. Shen, Transparent YAG ceramics by surface softening of nanoparticles in spark plasma sintering, Mater. Sci. Eng. A 429 (2006) 74–78.
[89] S. Rothe, S. Kalabukhov, N. Frage, S. Hartmann, Field assisted sintering technology. Part I: experiments, constitutive modeling and parameter identification, GAMM-Mitteilungen 39 (2016) 114–148.
[90] D.S.B. Heidary, M. Lanagan, C.A. Randall, Contrasting energy efficiency in various ceramic sintering processes, J. Eur. Ceram. Soc. (2017).
[91] A. Karakuscu, M. Cologna, D. Yarotski, J. Won, J.S. Francis, R. Raj, et al., Defect structure of flash-sintered strontium titanate, J. Am. Ceram. Soc. 95 (2012) 2531–2536.

[92] J.S. Francis, M. Cologna, D. Montinaro, R. Raj, Flash sintering of anode–electrolyte multilayers for SOFC applications, J. Am. Ceram. Soc. 96 (2013) 1352–1354.
[93] R. Todd, E. Zapata-Solvas, R. Bonilla, T. Sneddon, P. Wilshaw, Electrical characteristics of flash sintering: thermal runaway of Joule heating, J. Eur. Ceram. Soc. 35 (2015) 1865–1877.
[94] Y. Zhang, J.-I. Jung, J. Luo, Thermal runaway, flash sintering and asymmetrical microstructural development of ZnO and ZnO–Bi2O3 under direct currents, Acta Mater. 94 (2015) 87–100.
[95] R. Raj, M. Cologna, J.S. Francis, Influence of externally imposed and internally generated electrical fields on grain growth, diffusional creep, sintering and related phenomena in ceramics, J. Am. Ceram. Soc. 94 (2011) 1941–1965.
[96] M. Cologna, B. Rashkova, R. Raj, Flash Sintering of Nanograin Zirconia in < 5 s at 850 C, J. Am. Ceram. Soc. 93 (2010) 3556–3559.
[97] S. Ghosh, A.H. Chokshi, P. Lee, R. Raj, A huge effect of weak dc electrical fields on grain growth in zirconia, J. Am. Ceram. Soc. 92 (2009) 1856–1859.
[98] J. Obare, W.D. Griffin, H. Conrad, Effects of heating rate and DC electric field during sintering on the grain size distribution in fully sintered tetragonal zirconia polycrystals stabilized with 3% molar yttria (3Y-TZP), J. Mater. Sci. 47 (2012) 5141–5147.
[99] S. Šturm, A. Benčan, M.A. Gulgun, B. Malič, M. Kosec, Determining the stoichiometry of (K, Na) NbO3 using optimized energy-dispersive X-ray spectroscopy and Electron energy-Loss spectroscopy analyses in a transmission Electron microscope, J. Am. Ceram. Soc. 94 (2011) 2633–2639.
[100] M. Yu, S. Grasso, R. Mckinnon, T. Saunders, M.J. Reece, Review of flash sintering: materials, mechanisms and modelling, Adv. Appl. Ceram. 116 (2017) 24–60.
[101] K. Vanmeensel, A. Laptev, J. Hennicke, J. Vleugels, O. Van der Biest, Modelling of the temperature distribution during field assisted sintering, Acta Mater. 53 (2005) 4379–4388.
[102] B. Qian, Z. Shen, Laser sintering of ceramics, J. Asian Ceram. Soc. 1 (2013) 315–321.
[103] F.-H. Liu, Synthesis of biomedical composite scaffolds by laser sintering: mechanical properties and in vitro bioactivity evaluation, Appl. Surf. Sci. 297 (2014) 1–8.
[104] A. Sandmann, C. Notthoff, M. Winterer, Continuous wave ultraviolet-laser sintering of ZnO and TiO2 nanoparticle thin films at low laser powers, J. Appl. Phys. 113 (2013) 044310.
[105] A. Franco, L. Romoli, Characterization of laser energy consumption in sintering of polymer based powders, J. Mater. Process. Technol. 212 (2012) 917–926.
[106] J.-P. Kruth, L. Froyen, J. Van Vaerenbergh, P. Mercelis, M. Rombouts, B. Lauwers, Selective laser melting of iron-based powder, J. Mater. Process. Technol. 149 (2004) 616–622.
[107] K. Shahzad, J. Deckers, S. Boury, B. Neirinck, J.-P. Kruth, J. Vleugels, Preparation and indirect selective laser sintering of alumina/PA microspheres, Ceram. Int. 38 (2012) 1241–1247.
[108] L. Lü, J. Fuh, Y.-S. Wong, Laser-Induced Materials and Processes for Rapid Prototyping, Springer Science & Business Media, 2013.
[109] S. Failla, C. Melandri, L. Zoli, G. Zucca, D. Sciti, Hard and easy sinterable B4C-TiB2-based composites doped with WC, J. Eur. Ceram. Soc. 38 (2018) 3089–3095.
[110] K. Dai, L. Shaw, Thermal and mechanical finite element modeling of laser forming from metal and ceramic powders, Acta Mater. 52 (2004) 69–80.
[111] R.R. Gattass, E. Mazur, Femtosecond laser micromachining in transparent materials, Nat. Photonics 2 (2008) 219.
[112] P. Regenfuss, A. Streek, L. Hartwig, S. Klötzer, T. Brabant, M. Horn, et al., Principles of laser micro sintering, Rapid Prototyp. J. 13 (2007) 204–212.
[113] R. Sreenivasan, A. Goel, D.L. Bourell, Sustainability issues in laser-based additive manufacturing, Phys. Procedia 5 (2010) 81–90.
[114] R. Paul, S. Anand, Process energy analysis and optimization in selective laser sintering, J. Manuf. Syst. 31 (2012) 429–437.
[115] J.-P. Kruth, P. Mercelis, J. Van Vaerenbergh, L. Froyen, M. Rombouts, Binding mechanisms in selective laser sintering and selective laser melting, Rapid Prototyp. J. 11 (2005) 26–36.
[116] B. Staniewicz-Brudnik, A. Stwora, G. Skrabalak, E. Bączek, J. Maszybrocka, The technique of selective laser sintering (SLS) in the design high-porous ceramic implants, Mechanik 89 (2016) 540–1.
[117] C. Bowen, J. Open, J. Fitzmaurice, S. Mahon, Fast firing of electroceramics, Ferroelectrics 228 (1999) 159–166.
[118] C.-C. Hsueh, M.L. Mecartney, W.B. Harrison, M. Renee, B. Hanson, B.G. Koepke, Microstructure and electrical properties of fast-fired lead zirconate-titanate ceramics, J. Mater. Sci. Lett. 8 (1989) 1209–1216.
[119] C.E. Baumgartner, Fast firing and conventional sintering of lead zirconate titanate ceramic, J. Am. Ceram. Soc. 71 (1988) C-350-C-3.
[120] M. Harmer, R. Brook, Fast firing- microstructural benefits, Trans. J. Br. Ceram. Soc. 80 (1981) 147.
[121] H. Mostaghaci, R. Brook, Microstructure development and dielectric properties of fast-fired BaTiO 3 ceramics, J. Mater. Sci. 21 (1986) 3575–3580.
[122] D.H. Kim, C.H. Kim, Effect of heating rate on pore shrinkage in yttria-doped zirconia, J. Am. Ceram. Soc. 76 (1993) 1877–1878.
[123] S. Gómez, A. Da Silva, D. Gouvêa, Castro RHRd, D. Hotza, Nanocrystalline yttria-doped zirconia sintered by fast firing, Mater. Lett. 166 (2016) 196–200.
[124] A. Klein, D. Hotza, Advanced ceramics with dense and fine-grained microstructures through fast firing, Rev. Adv. Mater. Sci. 30 (2012) 273–281.
[125] D.E. García, D. Hotza, R. Janssen, Building a sintering front through fast firing, Int. J. Appl. Ceram. Technol. 8 (2011) 1486–1493.
[126] I. Bershitskii, A. Skochilov, N. Belyakova, V. Korovina, R. Avedin, S. Mirskii, Small electric furnaces for producing thermal insulating materials and ferrous alloys, Refract. Ind. Ceram. 48 (2007) 46–48.
[127] M. Barbouche, M. Hajji, H. Ezzaouia, Electric arc furnace design and construction for metallurgical and semiconductor research, Int. J. Adv. Manuf. Technol. 82 (2016) 997–1006.
[128] M.N. Rahaman, Ceramic Processing and Sintering, CRC press, 2003.
[129] R.M. German, P. Suri, S.J. Park, Liquid phase sintering, J. Mater. Sci. 44 (2009) 1–39.
[130] R.M. German, Liquid Phase Sintering, Springer Science & Business Media, 2013.
[131] W. Kaysser, G. Petzow, Liquid phase sintering of ceramics, Emergent Process Methods for High-Technology Ceramics, Springer, 1984, pp. 225–231.
[132] T. Kimura, Q. Dong, S. Yin, T. Hashimoto, A. Sasaki, T. Sato, Synthesis and piezoelectric properties of Li-doped BaTiO3 by a solvothermal approach, J. Eur. Ceram. Soc. 33 (2013) 1009–1015.
[133] J. Guo, A.L. Baker, H. Guo, M. Lanagan, C.A. Randall, Cold sintering process: a new era for ceramic packaging and microwave device development, J. Am. Ceram. Soc. 100 (2017) 669–677.
[134] S. Funahashi, H. Guo, J. Guo, A.L. Baker, K. Wang, K. Shiratsuyu, et al., Cold sintering and co-firing of a multilayer device with thermoelectric materials, J. Am. Ceram. Soc. 100 (2017) 3488–3496.
[135] D. Goldman, E. Gutmanas, Effect of heat treatments on cold sintering of 410 l stainless steel, Powder Metall Int. 17 (1985) 269–272.
[136] D. Goldman, E. Gutmanas, D. Zak, Reduction of oxides and cold sintering of water-atomized powders of Ni, Ni-20Cr and Nimonic 80A, J. Mater. Sci. Lett. 4 (1985) 1208–1212.
[137] E. Gutmanas, Cold sintering under high pressure–mechanisms and application, Powder Metall Int. (1983) 129–132.
[138] E. Gutmanas, High-pressure compaction and cold sintering of stainless steel powders, Powder Met. Int. 12 (1980) 178–183.
[139] S. Funahashi, J. Guo, H. Guo, K. Wang, A.L. Baker, K. Shiratsuyu, et al., Demonstration of the cold sintering process study for the densification and grain growth of ZnO ceramics, J. Am. Ceram. Soc. 100 (2017) 546–553.
[140] S.-C. Liao, Y.-J. Chen, B. Kear, W. Mayo, High pressure/low temperature sintering of nanocrystalline alumina, Nanostructured Mater. 10 (1998) 1063–1079.
[141] D.M. Roy, G.R. Gouda, Porosity-strength relation in cementitious materials with very high strengths, J. Am. Ceram. Soc. 56 (1973) 549–550.
[142] S.I. HIRANO, S. Somiya, Hydrothermal reaction sintering of pure Cr2O3, J. Am. Ceram. Soc. 59 (1976) 534-.
[143] K. Anagisawa, M. Sasaki, M. Nishioka, K. Ioku, N. Yamasaki, Preparation of sintered compacts of anatase by hydrothermal hot-pressing, J. Mater. Sci. Lett. 13 (1994) 765–766.
[144] N. Yamasaki, K. Yanagisawa, M. Nishioka, S. Kanahara, A hydrothermal hot-pressing method: apparatus and application, J. Mater. Sci. Lett. 5 (1986) 355–356.
[145] J.-H. Kim, K. Yanagisawa, A. Onda, E. Sasabe, T. Yamamoto, Densification behavior of hydroxyapatite green pellets prepared by different methods, J. Ceram. Soc. Jpn. 123 (2015) 1097–1101.
[146] R.E. Riman, W.L. Suchanek, M.M. Lencka, Hydrothermal Crystallization of Ceramics. Annales de Chimie Science des Materiaux, Elsevier, 2002, pp. 15–36.
[147] D. Andeen, L. Loeffler, N. Padture, F. Lange, Crystal chemistry of epitaxial ZnO on (1 1 1) MgAl2O4 produced by hydrothermal synthesis, J. Cryst. Growth 259 (2003) 103–109.
[148] K. Kajiyoshi, N. Ishizawa, M. Yoshimura, Preparation of tetragonal barium titanate thin film on titanium metal substrate by hydrothermal method, J. Am. Ceram. Soc. 74 (1991) 369–374.
[149] Z. Shen, Z. Zhao, H. Peng, M. Nygren, Formation of tough interlocking microstructures in silicon nitride ceramics by dynamic ripening, Nature 417 (2002) 266.
[150] R. Chaim, A. Shlayer, C. Estournes, Densification of nanocrystalline Y2O3 ceramic powder by spark plasma sintering, J. Eur. Ceram. Soc. 29 (2009) 91–98.
[151] Z. Valdez-Nava, S. Guillemet-Fritsch, C. Tenailleau, T. Lebey, B. Durand, J.-Y. Chane-Ching, Colossal dielectric permittivity of BaTiO 3-based nanocrystalline ceramics sintered by spark plasma sintering, J. Electroceramics 22 (2009) 238–244.
[152] A. Ragulya, Rate-controlled synthesis and sintering of nanocrystalline barium titanate powder, Nanostructured Mater. 10 (1998) 349–355.
[153] I.-W. Chen, X.-H. Wang, Sintering dense nanocrystalline ceramics without final-stage grain growth, Nature 404 (2000) 168.
[154] Y. Takano, H. Takeya, H. Fujii, H. Kumakura, T. Hatano, K. Togano, et al., Superconducting properties of MgB 2 bulk materials prepared by high-pressure sintering, Appl. Phys. Lett. 78 (2001) 2914–2916.
[155] A. Polotai, K. Breece, E. Dickey, C. Randall, A. Ragulya, A novel approach to sintering nanocrystalline barium titanate ceramics, J. Am. Ceram. Soc. 88 (2005) 3008–3012.
[156] S. Sōmiya, Hydrothermal preparation and sintering of fine ceramic powders, MRS Online Proceedings Library Archive, (1983), p. 24.
[157] H. Kähäri, M. Teirikangas, J. Juuti, H. Jantunen, Dielectric properties of lithium molybdate ceramic fabricated at room temperature, J. Am. Ceram. Soc. 97 (2014) 3378–3379.
[158] J.-P. Maria, X. Kang, R.D. Floyd, E.C. Dickey, H. Guo, J. Guo, et al., Cold sintering: current status and prospects, J. Mater. Res. 32 (2017) 3205–3218.
[159] H. Guo, A. Baker, J. Guo, C.A. Randall, Protocol for ultralow-temperature ceramic sintering: an integration of nanotechnology and the cold sintering process, ACS Nano 10 (2016) 10606–10614.
[160] H. Guo, J. Guo, A. Baker, C.A. Randall, Cold sintering process for ZrO2-based ceramics: significantly enhanced densification evolution in yttria-doped ZrO2, J. Am. Ceram. Soc. 100 (2017) 491–495.
[161] D. Wang, H. Guo, C.S. Morandi, C.A. Randall, S. Trolier-McKinstry, Cold sintering and electrical characterization of lead zirconate titanate piezoelectric ceramics, APL Mater. 6 (2018) 016101.

[162] A. Kobata, K. Kusakabe, S. Morooka, Growth and transformation of TiO2 crystallites in aerosol reactor, AIChE J. 37 (1991) 347–359.
[163] B. Buesser, A.J. Gröhn, S.E. Pratsinis, Sintering rate and mechanism of TiO2 nanoparticles by molecular dynamics, J. Phys. Chem. C 115 (2011) 11030–11035.
[164] P.G. Hill, P.G. Hill, C.R. Peterson, Mechanics and Thermodynamics of Propulsion, Addison-Wesley Pub. Co., 1965.
[165] T.L. Bergman, F.P. Incropera, Fundamentals of Heat and Mass Transfer, John Wiley & Sons, 2011.
[166] A. Bejan, Convection Heat Transfer, John Wiley & Sons, 2013.
[167] F. Kesicki, N. Strachan, Marginal abatement cost (MAC) curves: confronting theory and practice, Environ. Sci. Policy 14 (2011) 1195–1204.
[168] A. Vogt-Schilb, S. Hallegatte, Marginal abatement cost curves and the optimal timing of mitigation measures, Energy Policy 66 (2014) 645–653.
[169] D. Toke, S. Taylor, Demand reduction in the UK—with a focus on the non-domestic sector, Energy Policy 35 (2007) 2131–2140.
[170] T. Ibn-Mohammed, R. Greenough, S. Taylor, L. Ozawa-Meida, A. Acquaye, Integrating economic considerations with operational and embodied emissions into a decision support system for the optimal ranking of building retrofit options, Build. Environ. 72 (2014) 82–101.
[171] S. Taylor, The ranking of negative-cost emissions reduction measures, Energy Policy 48 (2012) 430–438.
[172] T. Ibn-Mohammed, R. Greenough, S. Taylor, L. Ozawa-Meida, A. Acquaye, Operational vs. embodied emissions in buildings—a review of current trends, Energy Build. 66 (2013) 232–245.
[173] M. Gorgolewski, Optimising renovation strategies for energy conservation in housing, Build. Environ. 30 (1995) 583–589.
[174] F. Levihn, On the problem of optimizing through least cost per unit, when costs are negative: implications for cost curves and the definition of economic efficiency, Energy 114 (2016) 1155–1163.
[175] J.L. Ponz-Tienda, A.V. Prada-Hernández, A. Salcedo-Bernal, The problem of ranking CO 2 abatement measures: a methodological proposal, Sustain. Cities Soc. 26 (2016) 306–317.
[176] T. Ibn-Mohammed, L. Koh, A. Acquaye, S. Taylor, A Robust Model to Enhance Organisation Boardrooms' Decision-Making Process Towards a Low Carbon Economy. Sustainable Future Energy Technology and Supply Chains, Springer, 2015, pp. 3–24.
[177] M. Pavan, R. Todeschini, Total-order ranking methods, Data Handl. Sci. Technol. 27 (2008) 51–72.
[178] Y.R. Zhang, T. Nayak, H. Hong, W. Cai, Biomedical applications of zinc oxide nanomaterials, Curr. Mol. Med. 13 (2013) 1633–1645.
[179] A. Moezzi, A.M. McDonagh, M.B. Cortie, Zinc oxide particles: synthesis, properties and applications, Chem. Eng. J. 185 (2012) 1–22.
[180] T. Ibn-Mohammed, I. Reaney, S. Koh, A. Acquaye, D. Sinclair, C. Randall, et al., Life cycle assessment and environmental profile evaluation of lead-free piezoelectrics in comparison with lead zirconate titanate, J. Eur. Ceram. Soc. (2018).
[181] A. Aimable, H. Goure Doubi, M. Stuer, Z. Zhao, P. Bowen, Synthesis and sintering of ZnO nanopowders, Technologies 5 (2017) 28.
[182] T. Ibn-Mohammed, S. Koh, I. Reaney, A. Acquaye, D. Wang, S. Taylor, et al., Integrated hybrid life cycle assessment and supply chain environmental profile evaluations of lead-based (lead zirconate titanate) versus lead-free (potassium sodium niobate) piezoelectric ceramics, Energy Environ. Sci. 9 (2016) 3495–3520.
[183] H.T. Kim, Y.H. Han, Sintering of nanocrystalline BaTiO3, Ceram. Int. 30 (2004) 1719–1723.
[184] Y.J. Wu, J. Li, R. Kimura, N. Uekawa, K. Kakegawa, Effects of preparation conditions on the structural and optical properties of spark plasma-sintered PLZT (8/65/35) ceramics, J. Am. Ceram. Soc. 88 (2005) 3327–3331.
[185] F. Zuo, A. Badev, S. Saunier, D. Goeuriot, R. Heuguet, S. Marinel, Microwave versus conventional sintering: estimate of the apparent activation energy for densification of α-alumina and zinc oxide, J. Eur. Ceram. Soc. 34 (2014) 3103–3110.
[186] M.V. Ramana, S.R. Kiran, N.R. Reddy, K.S. Kumar, V. Murthy, B. Murty, Investigation and characterization of Pb (Zr0. 52Ti0. 48) O3 nanocrystalline ferroelectric ceramics: by conventional and microwave sintering methods, Mater. Chem. Phys. 126 (2011) 295–300.
[187] C. Schmerbauch, J. Gonzalez-Julian, R. Röder, C. Ronning, O. Guillon, Flash sintering of nanocrystalline zinc oxide and its influence on microstructure and defect formation, J. Am. Ceram. Soc. 97 (2014) 1728–1735.
[188] X. Su, G. Bai, Y. Jia, Z. Wang, W. Wu, X. Yan, et al., Flash sintering of lead zirconate titanate (PZT) ceramics: influence of electrical field and current limit on densification and grain growth, J. Eur. Ceram. Soc. 38 (2018) 3489–3497.
[189] J.-C. M'Peko, J.S. Francis, R. Raj, Field-assisted sintering of undoped BaTiO3: microstructure evolution and dielectric permittivity, J. Eur. Ceram. Soc. 34 (2014) 3655–3660.
[190] T. Hayashi, T. Inoue, Y. Nagashima, J. Tomizawa, Y. Akiyama, Low-temperature sintering of PZT with LiBiO2 as a sintering aid, Ferroelectrics 258 (2001) 53–60.
[191] M. Adachi, N. Nishibe, T. Shiosaki, A. Kawabata, Liquid-phase-sintering of barium titanate and its modified ceramics with addition of Pb5Ge3O11, J. Appl. Phys. 22 (1983) 77.
[192] M. Mazaheri, Sintering of nanocrystalline zinc oxide via conventional sintering, two step sintering and hot pressing, Ceram Mater. 62 (2010) 506–509.
[193] K. Ewsuk, G. Messing, Densification of sintered lead zirconate titanate by hot isostatic pressing, J. Mater. Sci. 19 (1984) 1530–1534.
[194] Y. Hirata, A. Nitta, S. Sameshima, Y. Kamino, Dielectric properties of barium titanate prepared by hot isostatic pressing, Mater. Lett. 29 (1996) 229–234.
[195] E. Worrell, S. Ramesohl, G. Boyd, Advances in energy forecasting models based on engineering economics, Annu. Rev. Environ. Resour. 29 (2004) 345–381.